

Isolation and characterization of CNC from waste maize cob available in Bangladesh as a potential candidate for the fabrication of multifunctional bio-nanocomposites: A new approach



Shamim Dewan ^b , Md. Mahmudur Rahman ^{a,*} , Md. Ismail Hossain ^a, Bijoy Chandra Ghos ^a, M Mohinur Rahman Rabby ^b, Md. Abdul Gafur ^c, Md. Al-Amin ^a, Md. Ashraful Alam ^d

^a BCSIR, Rajshahi Laboratory, Bangladesh Council of Scientific and Industrial Research (BCSIR), Rajshahi 6206, Bangladesh

^b Department of Chemical Engineering, Rajshahi University of Engineering and Technology (RUET), Rajshahi 6204, Bangladesh

^c Pilot Plant and Process Development Centre, Bangladesh Council of Scientific and Industrial Research (BCSIR), Dhaka 1205, Bangladesh

^d Institute of Glass and Ceramic Research & Testing (IGCRT), Bangladesh Council of Scientific and Industrial Research (BCSIR), Dhaka 1205, Bangladesh

ARTICLE INFO

Keywords:

Maize cob
Lignocellulosic fiber
Chemical modification
Sustainable environment
Bio polysaccharide
Potential reinforcement

ABSTRACT

Nano-cellulose is a biodegradable polysaccharide which has multifunctional uses due to its fascinating properties (i.e., antibacterial, antifungal, anticarcinogenic activity) in wastewater treatment, drug design, food packaging, etc. CNC usually extracted from primary plant (such as jute, hemp, flax, cotton, etc.) which has other significant uses (for example preparation of yarn, rope, tissue paper, etc.). To reduce the pressure on primary plant the use of waste biomass of secondary plant could be an effective and economic route of CNC isolation. In this study a series of chemical treatment i.e. scouring (5% soap solution), alkali treatment (16% NaOH solution), bleaching (2% NaClO₂ and 2% Na₂S₂O₅ solution at pH = 4.0), acid hydrolysis (60% H₂SO₄) was conducted to isolate CNC from the waste maize cob. Characterization of the specimens were conducted by FTIR-ATR (Fourier Transform Infrared-Attenuated Total Reflection), FESEM (Field Emission Scanning Electron Microscopy), XRD (X-ray Diffraction), EDX (Energy Dispersive X-ray), DLS (Dynamic Light Scattering), Thermal analysis (TGA/DTG/DTA), and Zeta potential analysis. Different functional groups (>C=O, C≡C, C-O-C, C-O, -OH, etc.) were identified by FTIR-ATR. Crystal structure, crystallite size, and crystallinity index of CNC (around 84.63±0.03%) were observed by XRD analysis. Produced CNC showed enhanced thermal stabilities in TGA/DTG/DTA curves (about 40% residual mass at 600 °C) with the appearance of a peculiar 2D honey comb like void surface microstructure in FESEM micrographs and the surface charge (around -7.09mV) was measured by zeta potential. The newly produced CNC was perfectly nano sized (around 100 nm according to DLS analysis and FESEM micrograph). Hence, this newly produced CNC would be beneficially used to fabricate bio-nanocomposites for potential applications in various sectors such as biomedical, engineering, and industrial wastewater treatment as an appropriate substitute of the unsafe fossil based synthetic ones to develop legitimate environment.

1. Introduction

Cellulose is a biopolymer which is very much available on earth (Rahman et al., 2018a; Rahman et al., 2024a; Hossain et al., 2024). The fundamental structural element of all plant fibers is cellulose. The building blocks of cellulose molecules are glucose units connected in lengthy chains (β -1,4 glycoside linkages link the repeating units of D-anhydro glucose C₆H₁₁O₅), which are then connected in bundles known as microfibrils. The most abundant type of renewable organic matter on earth is cellulose. It is a carbohydrate polymer composed of

repeating β -D-glucose units (Cheran et al., 2022). The hydrogen bonds in cellulose control the crystallinity and consequently the physical characteristics of natural fibers (Komuraiah et al., 2014). Besides cellulose other two major constituents of plant fibers are hemicellulose and lignin as illustrated in Fig. 1. CNC (Crystalline Nano Cellulose) is the nano sized crystalline form of cellulose (length: 100 nm to 250 nm, diameter: 5 nm to 70 nm) (Teo et al., 2020) which is biodegradable, biocompatible, and beneficially used in bio-nanocomposites fabrication. CNCs are biopolymer which are attractive because of some interesting properties i.e., high thermal sustainability, insulation property (Septevani et al.,

* Corresponding author.

E-mail address: shamrat.acce@gmail.com (Md.M. Rahman).

2017), large surface area (Kondor et al., 2021), excellent surface morphology, high crystallinity (Deepa et al., 2011; Li et al., 2009), high porosity, biodegradability (Khan et al., 2020), chemical inertness, excellent stiffness, low density, high strength (Trache et al., 2020). CNC is getting popular day by day due to its promising properties i.e., optical transparency, biodegradability, environment friendly nature, low thermal expansion (Liu et al., 2016). That's why CNCs have vast applications (Corrêa et al., 2010; Sheltami et al., 2012; Shen et al., 2013; Li et al., 2015; Xie et al., 2019; Wang et al., 2020; Ren et al., 2022; Chaka, 2022). Scientists are now concerned with improving the sustainability and caliber of ecofriendly products in order to maintain the climate and biodiversity (Shelare et al., 2023; Soudagar et al., 2024a & 2024b & 2024d). Owing to their biodegradable qualities and environmentally beneficial practices, people are switching back to natural fibers from synthetic and potentially harmful materials. Having a lesser density than glass fiber they have been effectively utilized in the engineering and construction sectors. Use of natural fibers might help to reduce pollution and greenhouse gas emissions (Karimah et al., 2021; Hassan et al., 2024; Soudagar et al., 2024c). Different components are used in defined amounts to create the artificial fibers in certain ways. Globally, the synthetic fibers are same. For this reason, they have similar mechanical and thermal properties. Conversely, natural fibers are grown in a natural setting with the aid of soil, water, sunlight, and air that's why they have special qualities. Environmental circumstances differ from place to place and from season to season, and these differences have an impact on plant development. Therefore, they differ geographically in terms of their mechanical and thermal properties (Komuraiah et al., 2014). Maize cob contains a sufficient amount of cellulose (more than 40%) that can be used as a raw material for CNC (Sartika et al., 2023). Synthetic polymers (such as polyethylene, polyvinyl chloride, polyethylene terephthalate, etc.) are widely used as packaging materials (Rahman et al., 2024g; Kabir et al., 2018; Alojaly et al., 2022). They are not ecofriendly and responsible for environment pollution due to their non-biodegradable (Rydz, 2024) property. Synthetic polymeric materials don't undergo

natural decomposition i.e., bacterial decomposition and sustain as permanent waste (Eubeler et al., 2009) in the environment which are contaminating air, oceans, rivers, lands regularly. Combustion of the synthetic polymeric materials generate CO₂, CO, NO, NO₂, SO₂ (Żukowski et al., 2023) which are responsible for global warming, air pollution, acid rain, etc. Further, they enter into the ecosystem as microplastics resulting various desieses of human (such as cancer, cardiovascular disease, kidney failure, etc.) and animals (Zhao et al., 2023). Use of synthetic polymers could be replaced by biopolymers which are ecofriendly as well as easily undergo bacterial decomposition (Babaremu et al., 2023). CNC is a biopolymer which can be used in packaging, biomedical application like drug delivery, wound dressings, tissue engineering, antibacterial activity, biosensor, and bioimaging (Raghuvanshi & Garnier, 2024; Du et al., 2019; Lin & Dufresne, 2014), bio-nanocomposites fabrication (Khatun et al., 2023; Ulaganathan et al., 2022), etc. Wastewater treatment is one of the potential applications of fabricated bio-nanocomposites (Noreen et al., 2021). Wastewater treatment is a big challenge in different textile industry. Textile industries generally use different chemical treatment (Hayat et al., 2015) method for wastewater treatment which are at the same time very much costly and not ecofriendly (dengarous for aquatic life). Bio-nanocomposites fabricated from CNCs are cheap, ecofriendly material which has high efficiency in textile wastewater treatment (El Messaoudi et al., 2024; Rahman & Maniruzzaman, 2021; Rahman et al., 2022; Rahman et al., 2023b). Plants which are not cultivated for wood can be classified in two groups i.e., primary plants, secondary plants (Rahman et al., 2023c). Fiber producing plants such as jute, cotton, etc. are categorized as primary plants. On the other hand, plants which are cultivated basically for their stem, fruits, flowers while fiber is found as byproduct can be defined as secondary plants such as corn, okra, papaya, etc. CNC generally isolated from primary plants (Dhali et al., 2021). This is not an economic way of CNC extraction because primary plants have other significant uses. Isolation of CNC from the waste of secondary plants could be an economic route which at the same time

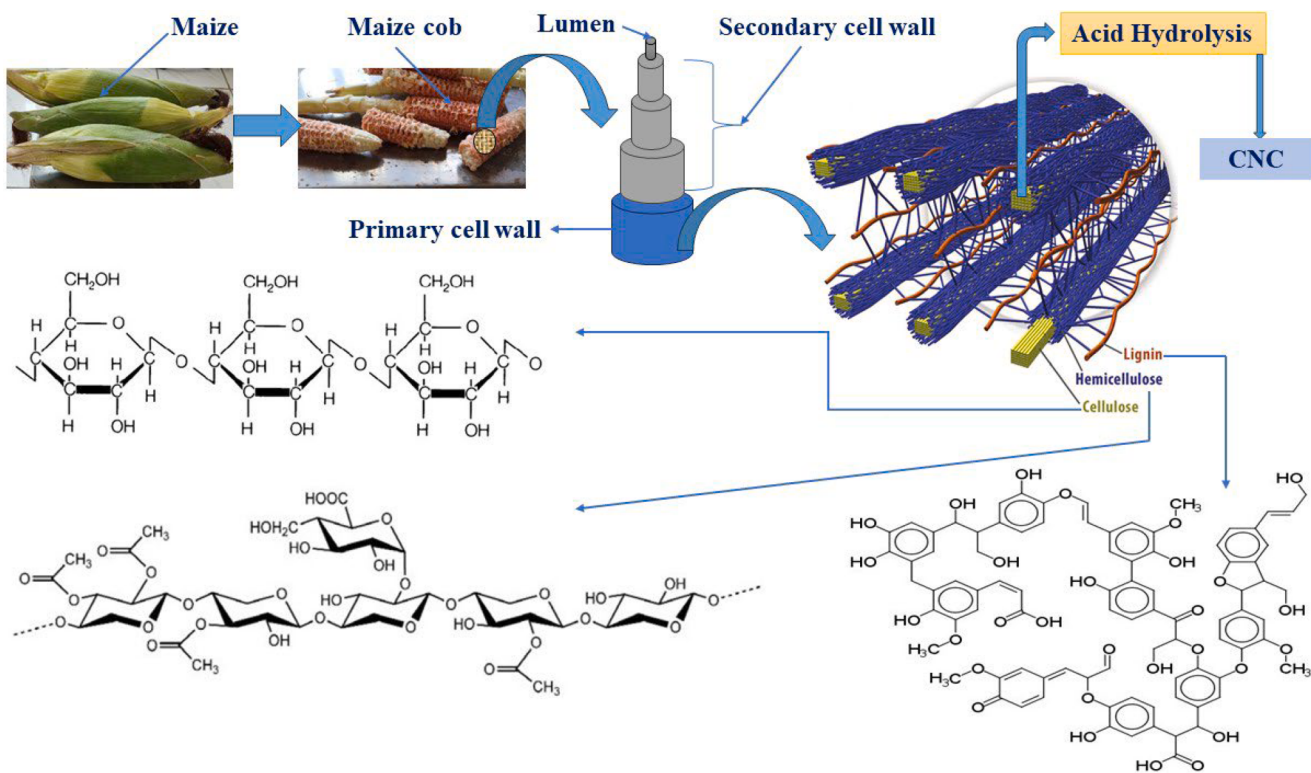


Fig. 1. Building structure of the lignocellulosic fiber of maize cob in the particular variety of maize (*Zea mays*) along with complex molecular structure of cellulose, hemicellulose, and lignin.

will reduce dependency on primary plants. The literature review says that CNCs have been extracted from different agro-industrial wastes such as corn husk (Kampeerapappun, 2015), rice straw (Lu et al., 2012), banana rachis (Sheikh et al., 2023; Rahman et al., 2024e), wheat straw (Pereira et al., 2017), bamboo fiber (Rasheed et al., 2020), pineapple crown (Prado et al., 2019), cotton pulp (Chen et al., 2019), cocoa pod husk (Akinjokun et al., 2021), sugarcane bagasse (Leão et al., 2017), coconut husk fibers (Poornachandhra et al., 2023), pea hull (Li et al., 2020). Maize (*Zea mays*) is a widely cultivated cereal product of grass family (Poaceae) (Perera, 2014). Comparison of the environmental and economic impact focusing on its major waste called maize cob, a source of CNC are shown in Fig. 11. Maize can broadly be classified in two major parts i.e., edible part, waste part. Waste part can further be classified in three parts i.e., maize shell, maize cob, silk. Waste part of the maize is valueless and useless one which is responsible for bad smell production during bacterial decomposition, drainage block in rainy season, and CO₂ emission during combustion. Maize cob, an agro-waste biomass could also be a potential source of cellulose to produce CNC due to its high amount of cellulose, hemicellulose and low amount of lignin as mentioned in Table 1. For why maize cob extracted fiber's application as nanocellulose is highly encouraged as it will reduce the burden of burning-off, resulting in environmental pollution of water and air (Rajanna et al., 2022).

In this study, CNC would be extracted from the purified fiber of waste maize cob by H₂SO₄ hydrolysis method. Before hydrolysis sequentially series of chemical treatment (i.e., scouring, alkali treatment, bleaching) to be performed for the purification of the fiber. A portion of work has been conducted to isolate CNC from the waste of secondary plant (particularly maize) but in previous no one has performed such work from the waste material particularly from the Bangladeshi variety maize cob namely *Z. mays* which is much more available in Rajshahi region. Additionally, the quality and the high yield of the obtained nanocellulose could be promising while their characterization could have been performed by conducting a number of useful technique namely FTIR-ATR, FESEM, XRD, EDX, DLS, TGA/DTG/DTA, and Zeta potential analysis. Hence, in this study, maize cob of Bangladeshi variety, a completely economically valueless and useless product has been selected to produce very much economically valuable product like CNC which has various potential uses. The prospects of this study are (i) to develop a new route of production of CNC from the agrowaste biomass of maize cob of Bangladeshi variety, and (ii) to optimize the overall thermomechanical, physicochemical, morphological properties of the newly produced CNC as a suitable reinforcement to fabricate biocomposites for potential applications in various sectors as an appropriate substitute of the unsafe fossil based synthetic ones to develop legitimate environment.

Table 1
Chemical constituents in terms of cellulose, hemicellulose, and lignin in different source based natural fibers.

Fiber source	Cellulose (%)	Hemicellulose (%)	Lignin (%)	References
Banana trunk	31.48	14.98	15.07	(Muthu et al., 2020; Karimah et al., 2021)
Kenaf	36	21	18	
Rice straw	30	25	15	
Wheat straw	35	28	18	
Barley straw	38	33	16	
Banana leaf	25.65	17.04	24.84	
Rice husk	40	22	20	
Sugarcane bagasse	40	25	15	
Maize cob (<i>Z. mays</i>)	52	28	15	This study

2. Experimental

2.1. Materials

Z. mays was collected from Shaheb Bazar, Rajshahi, Bangladesh which was the main raw material of this study. CNC was isolated particularly from its cob. Ghari detergent manufactured by RSPL Health BD LTD collected from a local market of Rajshahi, Bangladesh to prepare 5% soap solution. Sodium hydroxide (NaOH) pellets (with purity ≥ 97%) manufactured by Merck Specialities Private Limited (India), Sodium Chlorite (NaClO₂) fine powder (with purity 86~94%) manufactured by Research-Lab Fine Chem Industries (India), Sodium Metabisulphite (Na₂S₂O₅) fine powder (with purity 97~98%) manufactured by Research-Lab Fine Chem Industries (India), Hydrochloric acid (HCl) solution purity about 37% manufactured by Merck Life Science Private Limited (India), Sulfuric acid (H₂SO₄) purity about 98% manufactured by Supelco, Merck Darmstadt, Germany (analytical grade), distilled water and ultrapure water were prepared and collected from Biopolymers and Sustainable Environmental Research Laboratory, BCSIR Rajshahi.

2.2. Method

2.2.1. Collection of maize cob fiber

The particular variety of maize, *Z. mays* was collected from Rajshahi, Bangladesh. Then maize cob was manually separated from the maize. Later the raw fiber was prepared by mechanical hammer milling and blending method. Finally, the obtained raw maize cob fiber was dried in an oven at 105 °C and then stored in a sealed condition for further study. Workflow of fiber extraction from the waste maize cob after harvesting its edible parts have shown in Fig. 2.

2.2.2. Scouring

Scouring was conducted to remove different dusty, waxy, gummy, oily substances from the fiber. Scouring was carried out by 5% soap solution. The ratio of prepared maize cob fiber to solution of the 5% soap solution was 1:20 (Rahman et al., 2023c). The detergent solution with maize cob fiber then heated at a temperature of 60 °C. Maintaining that temperature scouring was performed for 2 hr with moderate stirring. After that, the fiber was repeatedly cleaned on a filter cloth using distilled water. Then the scoured fiber was dried in the oven (at 105 °C) and finally stored in a thumped condition (Rahman et al., 2022).

2.2.3. Alkali treatment

Alkali treatment of the scoured fiber was performed to draw out hemicellulose and lignin from the desired alpha cellulose (Sartika et al., 2023; Rahman et al., 2024c). Alkali treatment was carried out by using 16% NaOH solution. The ratio of scoured maize cob fiber to 16% NaOH solution was maintained at 1:20. The NaOH solution with scoured maize cob fiber was heated at 70 °C on a hot plate. Then the treatment was continued for 2h with moderate stirring (Rahman & Rahman, 2022; Rahman et al., 2024d). After being alkali treated, the fiber was repeatedly rinsed with distilled water. Washing was carried out on a filter cloth. Ultimately, the fiber that had been alkali treated was dried at 105 °C in an electric oven and stored in a moisture free condition until bleaching (Hassan et al., 2024; Sheikh et al., 2023).

2.2.4. Bleaching

Bleaching of the alkali treated fiber was conducted to obtain complete removal of the lignin of the bundle of fibers. Total bleaching process was carried out by 2% NaClO₂ solution and 2% Na₂S₂O₅ solution. The ratio of alkali treated maize cob fiber to 2% NaClO₂ solution was maintained at 1:20. pH of the solution was carefully maintained at 4 by using 0.1N HCl and 0.1N NaOH (Rahman et al., 2023b, Rahman et al., 2024a). Temperature of the mixture kept at 95 °C. Treatment of the fiber was conducted for 2h with moderate stirring. Later the fiber was

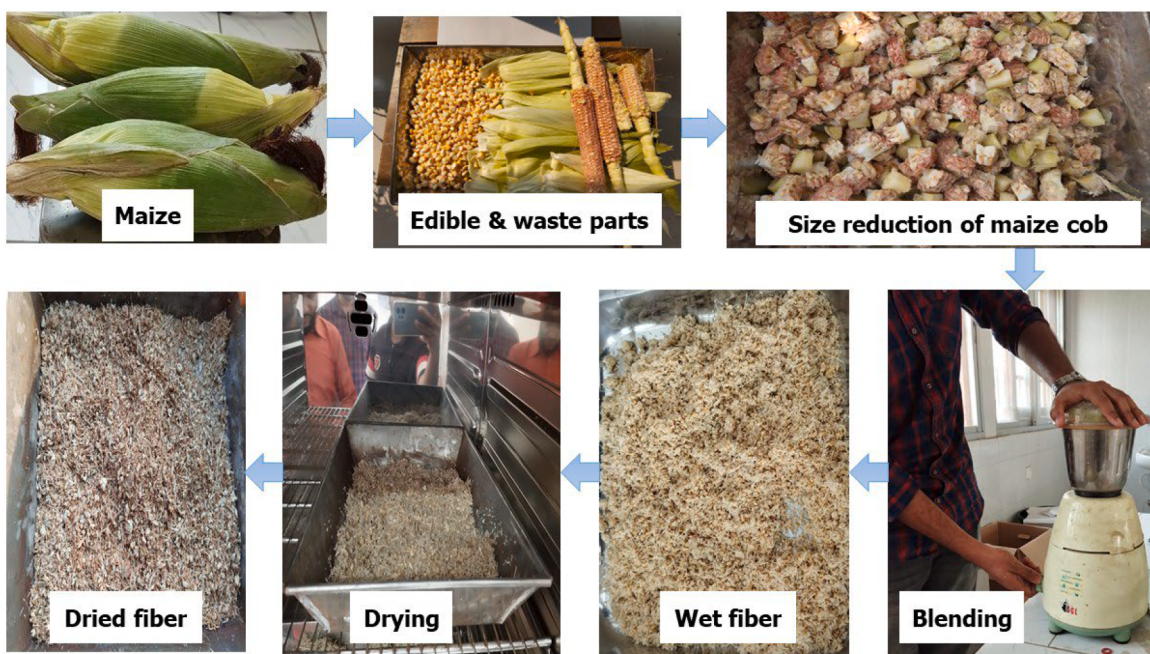


Fig. 2. Raw fiber extraction procedure during the experimental session from the waste maize cob of *Z. mays* by applying mechanical hemmer milling and blending process.

repeatedly washed by using distilled water. Then the fiber was further treated with 2% $\text{Na}_2\text{S}_2\text{O}_5$ solution where fiber to 2% $\text{Na}_2\text{S}_2\text{O}_5$ solution ratio was 1:30. The fiber was treated with 2% $\text{Na}_2\text{S}_2\text{O}_5$ solution at room temperature in a dark condition for thirty minutes (Sheikh et al., 2023; Hossain et al., 2024). After drying in the electric oven at 105 °C, the bleached fiber was finally rinsed several times on a filter cloth with

distilled water and kept in a thumped condition.

2.2.5. Sulfuric acid hydrolysis

For acid hydrolysis first of all bleached alpha cellulose was taken in small size (by cutting down as small as possible). Then CNC was extracted by acid hydrolysis of bleached small sized maize cob fiber. The

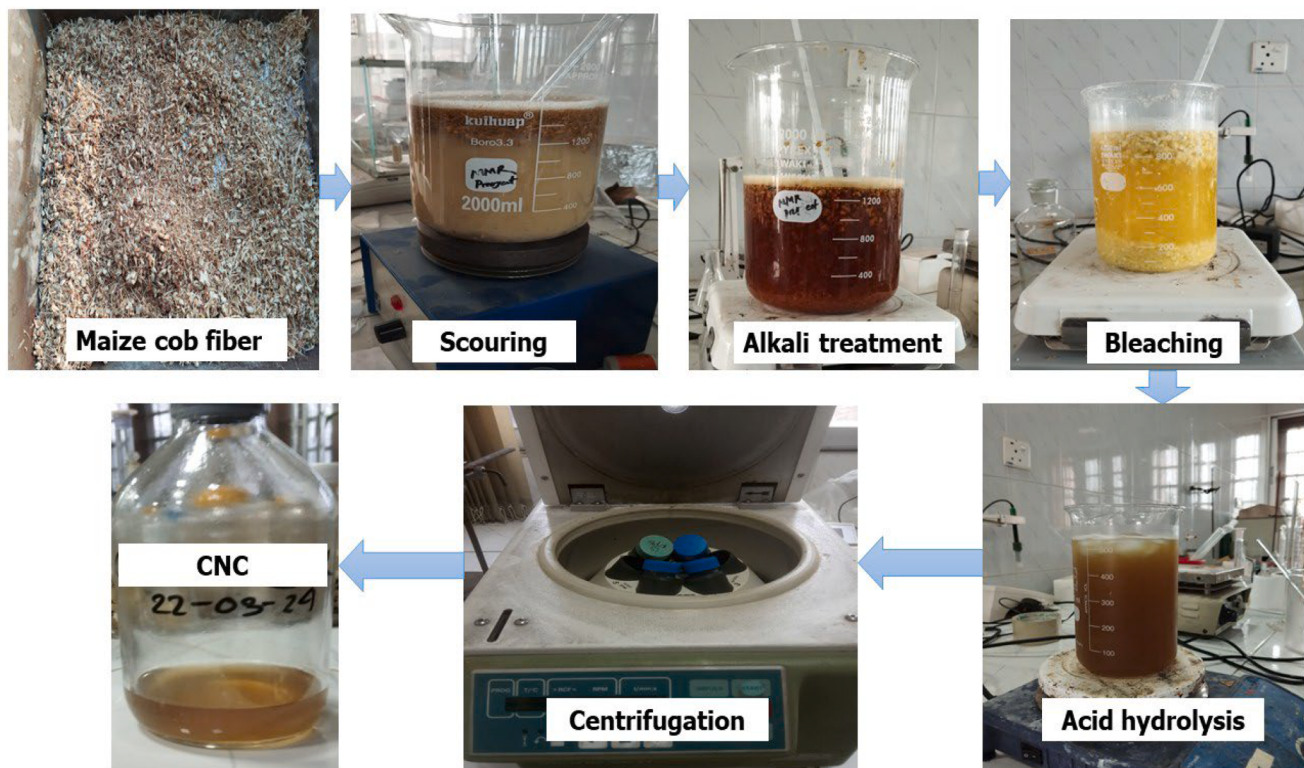


Fig. 3. Sequential CNC isolation processes (scouring, alkali treatment, bleaching, sulfuric acid hydrolysis, centrifugation respectively) from the extracted raw maize cob fiber, a secondary plant based agro-waste biomass.

hydrolysis was conducted by 60% H₂SO₄ solution under nonstop stirring with magnetic stirrer on a hot plate at 40 °C for 15 min (Sartika et al., 2023; Rahman et al., 2018a). During hydrolysis the fiber to 60% H₂SO₄ solution was maintained at 1:15 ratio. After 15 min, the reaction was quenched by ice and stirring was conducted for another 30 min. Later the suspension was diluted by distilled water and cooled down at room temperature. Then the suspended CNC was separated from the diluted suspension by centrifugation process (6000 rpm, 1 °C, 12 min) and the solid fraction was stored in 96% ethanol after totally neutralizing (pH=7.0) by distilled water (Hassan et al., 2024; Kusmono et al., 2020). Yield of CNC from maize cob typically ranges from 50–55% (Sartika et al., 2023) of the initial biomass, depending on the efficiency of the acid hydrolysis process whereas yield of CNC from traditional sources (e.g., jute, hemp) typically range from 60–65% (Kassab et al., 2020). Although the yield percent is higher in traditional sources (e.g., jute, hemp) but to achieve this high yield it is required higher quantity of chemicals for the isolation on the other hand it is possible to isolate CNC from maize cob in lower cost by limited chemicals use. Jute, hemp, etc. have some significant uses but maize cob is just an agro waste. As a waste material maize cob is responsible for environmental pollution that's why it must be beneficial if CNC is isolated from this waste. Workflow of CNC isolation elaborately illustrated in Fig. 3. All the experiments like scouring, alkali treatment, bleaching, and acid hydrolysis were conducted by maintaining/wearing Personal Protective Equipment (PPE) such as head cap, safety goggles, latex gloves, face mask, apron, safety shoes to avoid health distress since some harsh chemicals (NaOH, NaClO₂, Na₂S₂O₅, HCl, H₂SO₄) were used for the experimental purpose.

3. Characterization methods

3.1. FTIR-ATR analysis

FTIR-ATR technique is often used to inspect precisely the intramolecular and intermolecular interaction in polymeric specimens. FTIR spectroscopy also used to determine the presence of active sites or functional groups, chemical structure, chemical compositions, purity of compound, overall molecular behavior, the quantity of targeted molecules, etc. (Rahman et al., 2023c). PerkinElmer, Serial Number: 115, 061, Model: L1600300 spectrum Two made in Llantrisant, UK, was used for the functional group analysis among raw maize cob fiber, alkali treated fiber, bleached fiber, and maize cob CNC. The PerkinElmer was equipped with a high linearity room temperature DTGS detector and linked to PerkinElmer Spectrum IR software version 10.6.2. Specimen were placed to the ATR attachment of diamond prism, and using a resolution of 5 cm⁻¹ spectra were measured from 400 cm⁻¹ - 4000 cm⁻¹. Additionally, for each sample, minimum four replicas were taken for good observation (Rahman et al., 2023d).

3.2. FESEM analysis

The FESEM technique is frequently used for the morphological analysis of a particular surface of polymeric specimens (Orasugh et al., 2020). FESEM micrograph of the exposed chemically modified and unmodified natural fiber provides a clear suspicion about the microstructure, surface roughness, sorption profiling porosity, void structure, particle size, pore size, spiral structure, shrinkage or wrinkle, etc. By ImageJ and Origin Lab software, it is simple to determine the particle size and distribution curve from the SEM image. Using a vacuum sputter coater, a 200 Å gold coating was applied on the specimen in each analysis of raw fiber, alkali treated fiber, bleached fiber, and CNC to prevent them from charging onto the peripheral surface as well as for good quality image. For FESEM analysis the magnification range was kept around 10,000x - 30,000x. For this study to examine the samples a FESEM of model number (JEOL, Model: JSM-IT800, made in Japan) was used where accelerating voltage was 10kV to 20 kV (Rahman et al., 2023a and 2024f).

3.3. XRD analysis

XRD is a rapid analytical technique to perceive the crystalline nature of different polymeric specimens. In this study, the degree of crystallinity or crystallinity index of raw maize cob fiber, alkali treated fiber, bleached fiber, and maize cob CNC samples were measured by XRD analysis. BRUKER D8 ADVANCE wide angle X-ray diffractometer with 40 mA current, and Cu K α radiation ($\lambda = 0.154$ nm), 50 kV voltage, was used to inspect the specimens (Rahman and Maniruzzaman, 2024; Uddin et al., 2024; Rahman et al., 2018b). Varying the angle from 5° to 80° (20) the crystallinity index was detected. The crystallinity index (C_rI) can be calculated by the following equation:

$$C_{rI} = \frac{I_{CA}}{I_{CA} + I_{AM}} \times 100 \quad (1)$$

Where, I_{AM} and I_{CA} are the amorphous area and crystalline area respectively and they can easily be measured by the origin lab software (Bano & Negi, 2017).

The d-spacing can be calculated by using Bragg's equation:

$$n\lambda = 2dsin\theta \quad (2)$$

Here, λ is the X-ray wavelength, n is an integer, θ is the diffraction angle, and d is the distance between crystal lattice planes. Accurate crystallite size (L) can be calculated by the Scherrer equation:

$$L = \frac{0.94 \lambda}{H \cos \theta} \quad (3)$$

In this equation, H denotes the full width at half maximum of the peak in radians, λ is the X-ray wavelength (0.1542 nm), and θ stands for the Bragg angle (Benini et al., 2018; Hassan et al., 224).

3.4. Thermal analysis

A common method for evaluating the thermal stability brought on by the disintegration of different polymeric materials is thermogravimetric analysis, or TGA. The thermal analysis technique known as TGA is used to calculate the mass of a spacecraft in relation to time as temperature varies. Physical events like desorption and adsorption, phase transitions, and chemical phenomena like thermal breakdown, chemisorption, and solid gas reactions (reduction or oxidation) are all covered by this measurement. The sample is heated in a given environment (He, N₂, Air, Ar, CO₂, etc.) at constant rate in TGA analysis. As a function of temperature or time the change of weight of substance is recorded. During TGA analysis for a known initial weight of substance the temperature is increased at a constant rate and at different time interval as a function of temperature the changes in weights are recorded. The plot of weight change against temperature is called thermogram. The physical and chemical properties of polymeric specimens, as well as composition, melting and polymer relaxation temperatures, onset and maximum degradation temperatures, phase changes, type of chemical reaction occurring during the experiment, residual mass, etc. as a function of increasing heat, can all be determined by holding the heat constant up to 1000 °C (Loganathan et al., 2017; Rahman et al., 2023c). For thermal phase transitions, the first derivative of temperature is called DTA (Differential Thermal Analysis). The process of DTA involves monitoring a sample's thermal response as it is heated in order to analyze and determine the chemical composition of various substances. The method is based on the idea that heat causes reactions and phase changes in substances, which might result in the emission or absorption of heat (Wunderlich, 2001). DTG (Derivative Thermogravimetry) is the first derivative of TG. The rate of mass loss (dm/dT in mg/min unit) is given by the DTG peak height at any temperature (Karak, 2012). In this study thermal analysis of every specimen was conducted by a Thermal Gravimetric Analyser of model number (EXSTAR 6000 TG/DTA 6300, Seiko). Each specimen was taken in amounts of around 25 mg for

observation. The samples were heated gradually at a rate of 20 °C/min from 26 °C to 600 °C while maintaining a steady nitrogen flow rate of 60 ml/min (Rahman and Maniruzzaman, 2019; Hossain et al., 2024). To acquire the correct outcome, several analyses were performed for every sample.

3.5. DLS analysis

The size distribution profile of tiny particles in suspension or polymers in solution may be found using the DLS method. DLS is used to describe the size of different particles, such as micelles, vesicles, proteins, carbohydrates, and nanoparticles. It measures the hydrodynamic radius of particles. DLS is used to examine size range from a few nanometers to a few micrometers. The hydrodynamic radius of the nanoparticles is measured by the Stokes-Einstein equation.

$$D = \frac{K_B T}{6\pi\eta R} \quad (4)$$

Here, R is the radius of sphere, D is the diffusion constant, T is the absolute temperature, η is the dynamic viscosity, and K_B is the Boltzmann's constant. The speed at which the particles are diffusing because of Brownian motion is basically measured in DLS by measuring the intensity of the scattered light. Small particles cause the intensity to more fluctuate than larger. Main apparatuses of DLS are laser, detector. In DLS a laser i.e., He, Ne of known wavelength passes through a dilute sample. Using a detector intensity of scattered light is collected and based on collected scattered light particle size is determined. Correlogram of DLS analysis shows smooth curve in case of large particles and noisy curve in case of small particles. DLS analysis provides accurate result additionally turbid sample can be measured directly and another advantage is after measurement complete recovery of sample is possible. Some limitations of DLS analysis are it can't identify the size of solid particles (particles >1000 nm size are impossible to measure by this method), and it can measure the hydrodynamic radius of the particles and can't measure the actual size of particles (Mao et al., 2017; Patel et al., 2024; Loya et al., 2024). In this study, DLS analysis was conducted to identify the particle size of the isolated maize cob CNC. For nano particle size analysis HORIBA Scientific, nano partica, Nano Particle Analyzer, SZ-100V2 was used.

3.6. Zeta potential analysis

The charge that is located at the slipping point of a particle in a medium is called zeta potential. In other words, zeta potential analysis is used to measure the surface charge (both positive and negative) over a particle. Zeta potential is used to identify the stability of a colloid, to understand dispersion and aggregation process in water purification, paints and cosmetics, etc. Zeta potential is the potential which is observed at the shear plane. Zeta potential also known as electrokinetic potential that is basically the difference in the potential between electroneutral region of the solution and shear plane. Factors affecting zeta potential are pH, thickness, and concentration. Range of zeta potential typically from +100 to -100 mV. Zeta potential is measured by applying an electric field. Particles migrate toward the electrode of opposite charge in a particular velocity. The velocity of the particles depends on strength of electric field or voltage gradient. Zeta potential is associated with the electrophoretic mobility by the Henry equation. Electrophoretic mobility, μ_e is calculated from the equation:

$$\mu_e = \frac{V}{E} \quad (5)$$

Here, V is the particle velocity, E is the electric field strength. Once μ_e is calculated the zeta potential can be obtained by Henry's equation:

$$\mu_e = \frac{2 \varepsilon z f(Ka)}{3\eta} \quad (6)$$

Where, z is zeta potential, ε is dielectric constant, η is viscosity, and f(Ka) is the Henry's function (Bhattacharjee, 2016; Loya et al., 2024). In this study, zeta potential was applied to measure the surface charge of the isolated CNC. For zeta potential analysis HORIBA Scientific, nano partica, Nano Particle Analyzer, SZ-100V2 was used.

3.7. EDX analysis

The components or chemical content of the surface of natural polymers or biopolymeric composites have been extensively studied using EDX. This specific approach allows for the detection of various metals and minerals, including Pb, Cr, Cd, Zn, Na, Al, Si, Co, Cu, Mg, Ni, Ca, and others, along with the main chemical compositions and components that are often connected with the fiber's perimeter or structure, such as N, C, and O. Interestingly, even though hydrogen is one of the core components of biopolymers, this approach is unable to detect its existence or quantity because of its small size and the lack of electrons in its remotest shell (Ali, 2016; Moros et al., 2019; Nasrollahzadeh et al., 2019). In this study EDX analysis was performed to determine the components and their chemical compositions of raw maize cob fiber, bleached fiber, alkali treated fiber, and maize cob CNC. The analysis was conducted by the EDX analyzer of model QT-606 Energy dispersive X-ray fluorescence spectrometer RoHS1.0.

4. Result and discussion

4.1. FTIR-ATR analysis

FTIR spectroscopy is often used to examine the intramolecular and intermolecular hydrogen bonding among raw maize cob fiber, bleached fiber, alkali treated fiber, and maize cob CNC as FTIR is the most often used method for examining intramolecular and intermolecular interactions in polymers. In other words, FTIR spectroscopy gives clear indication about functional group. FTIR results of all the characterized specimen are mentioned in the Table 2 analyzing the wave number of Fig. 4. The peak at 3300 cm⁻¹ appeared among raw maize cob fiber, bleached fiber, alkali treated fiber, and maize cob CNC because of N-H stretching of amines (Rahman et al., 2018a; Hassan et al., 2024). In case of CNC, the peak (N-H) was sharp but raw, alkali treated, and bleached fiber provided small peak compared to CNC in FTIR analysis which indicates the successful CNC isolation. Because of C-H stretching the peak at 2850 cm⁻¹–2950 cm⁻¹ originated in FTIR analysis amongst isolated CNC, bleached fiber, alkali treated fiber, and raw fiber. A band at 2928 cm⁻¹ in the raw maize cob fiber caused by the aliphatic C-H bonds stretching (Costa et al., 2015). A Sharp peak was generated for CNC whereas raw, alkali treated, and bleached fiber provided small intensity peaks which implies successful chemical treatment during CNC isolation. Due to S-H stretching a peak of small intensity appeared at 2540 cm⁻¹ only for CNC. This new innovated peak may be because of efficacious acid hydrolysis during CNC isolation. The newly generated peak in CNC at a wave number of 2160 cm⁻¹ due to stretching of C≡C functional group. This alkyne group may be appeared because of a series of chemical treatments during CNC isolation. The peak at 1600–1900 cm⁻¹ was attributed to raw maize cob fiber, bleached fiber, alkali treated fiber, and maize cob CNC due to C=O stretching. Comparatively small peaks were found in that range among raw, alkali treated, and bleached fiber but the peak provided by CNC was sharp enough which specifies the perfect removal of impurities. Because of the symmetric bending of CH₂ functional group a peak at 1400–1450 cm⁻¹ appeared in case of raw maize cob fiber, bleached fiber, alkali treated fiber, and maize cob CNC. Comparing sharp and small intensity peaks it can be said that successful chemical treatment was conducted in each step of CNC isolation. In FTIR

Table 2

The most amenable functional groups with their particular intensity and wave number in case of raw fiber, alkali treated fiber, bleached fiber, and CNC.

Adsorption bond	Intensity	Raw fiber peak (cm^{-1})	Alkali treated fiber peak (cm^{-1})	Bleached fiber peak (cm^{-1})	CNC peak (cm^{-1})
-OH stretching	Sharp & Str.	3130–3500	3150–3550	3100–3600	3000–3750
N-H of Amines	Sharp & Str.	2800
C-H	Sharp & Str.	2710	2700	2715	2750
S-H	Broad & Str.	2540
C≡C	Broad & Str.	2160
C=O	Str.	1600	1630	1670	1700
C=O of Hemicellulose	Sharp & Str.	1720
CH ₂	Symmetric Bending	1420	1400	1433	1450
C-O	Str.	1325	1310	1260	1350
C-O-C	Sharp & Str.	1110	1090	1100	1150
C-OH of Lignin	Symmetric str.	1020	1030
C-H of Aromatics	Sharp & Str.	848	843	845	850
N-O	Str.	808	815	810	800
C-C Deformation	Bending	735
C-Cl	Sharp & Str.	600
S-S	Sharp & Str.	420

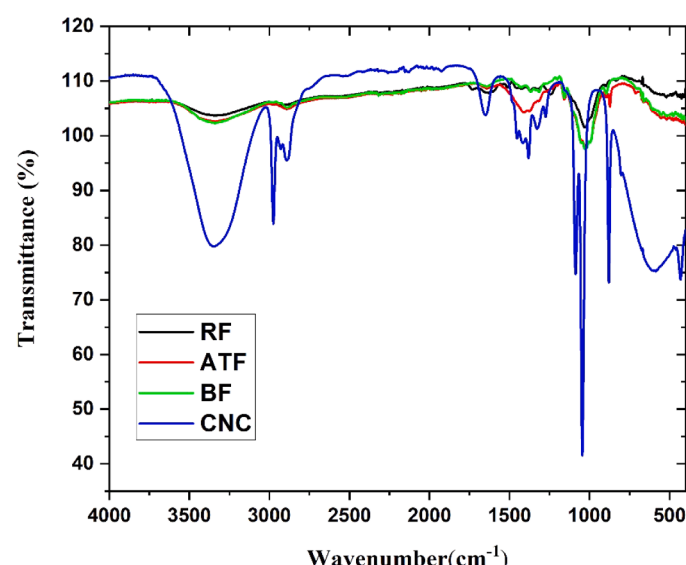


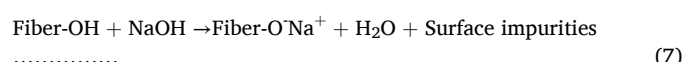
Fig. 4. The respective spectrum (in the range of 4000 to 400 cm^{-1}) of raw fiber, alkali treated fiber, bleached fiber, and maize cob derived CNC detected in FTIR-ATR analysis.

analysis of alkali-treated fiber between 1720–1740 cm^{-1} no peak appeared which specifies perfect removal of C=O group of hemicellulose from the fiber after alkali treatment (Rahman et al., 2023c). Comparing the alkali treated fiber with the raw fiber it can be claimed that the alkali treated fiber was pure and hemicellulose free. A sharp peak was noticed at 1260–1350 cm^{-1} in case of maize cob CNC because of C-O stretching. But the originated peak intensity at 1260–1350 cm^{-1} was not that sharp among raw, alkali treated, and bleached fiber. The sharp peak in CNC appeared due to its appropriate isolation. The peak attributed at 1070–1150 cm^{-1} for C-O-C stretching. In case of CNC sharp peak originated due to C-O-C stretching compared to raw, alkali treated, and bleached fiber in FTIR analysis. The sharp intensity peak appeared in CNC dictates its proper separation. The broad peak at 1020 cm^{-1} in raw fiber points to the presence of the C-OH group of lignin. The peak intensity reduced after alkali treatment that indicates removal of moderate amount of lignin during alkali treatment. No peak appeared due to C-OH group stretching of lignin in case of CNC and bleached fiber that dictates the successful removal of bundle of lignin during bleaching process hence it can be claimed that isolated CNC was totally lignin free. Though small intensity peaks appeared for raw, alkali treated, and bleached fiber but CNC provided a sharp peak that originated at 850 cm^{-1} because of C-H stretching of aromatics. Another peak of small intensity noticed at

800 cm^{-1} for N-O stretching in case of CNC but no peak attributed at that wave number for raw, alkali treated, and bleached fiber (Rahman et al., 2024b). This newly generated peak at 800 cm^{-1} for N-O stretching in CNC might be appeared because of chemical modification at that specific wavelength. Although no peak attributed in raw fiber but a small peak originated at 735 cm^{-1} due to C-C deformation in raw maize cob fiber, bleached fiber, alkali treated fiber which pointing the successful chemical treatment throughout the CNC isolation process. In CNC the newly generated peak at 600 cm^{-1} noticed due to C-Cl vibration. Raw, alkali treated, and bleached fiber didn't provide any peak at that wave number. A small and sharp peak also noticed at the wave number of 420 cm^{-1} because of S-S vibration in raw fiber and CNC respectively but bleached and alkali treated fiber did not give any vibration at that wave number. This phenomenon indicates that in raw fiber sulphur may be appeared from the air or soil and the alkali treatment, the bleaching process was removed that sulphur which came from soil or air. Further generation of the peak at 420 cm^{-1} due to S-S vibration in CNC might be attributed because of chemical modification of sulphur during H_2SO_4 hydrolysis (Sheikh et al., 2023). From the FTIR analysis, it is noticed that many functional groups were disappeared after CNC isolation although they were present in raw, alkali treated, and bleached fiber and many functional groups provided sharp peaks in CNC compared to raw, alkali treated, and bleached fiber again many functional groups were newly generated in CNC after isolation. Based on these phenomena it can be claimed that pure CNC was isolated from the raw fiber of maize cob through a series of chemical treatments.

4.2. FESEM analysis

FESEM analysis was conducted to inspect the morphological changes during different stages of purification by chemical treatment. Fig. 5 (a), The FESEM micrograph of raw maize cob fiber clearly showed the presence of different fatty, waxy, and gummy materials. The micrograph also demonstrated that the intercellular space of raw maize cob fiber was filled by lignin and fatty substances which hold the unit cells. Compared to the raw maize cob fiber with 16% NaOH treated fiber it appears that surface of the raw fiber roughened after alkali treatment as well as different impurities, fatty, waxy, and gummy substances successfully removed additionally porosity on the fiber surface was arrived. Fig. 5 (b), The FESEM micrograph of NaOH treated fiber dictates that NaOH treatment of the cellulose fiber increased the amount of amorphous cellulose (Rahman et al., 2022). Removal of hydrogen bond in the network structure which was an important alteration that occurred due to NaOH treatment according to the following reaction stoichiometry:



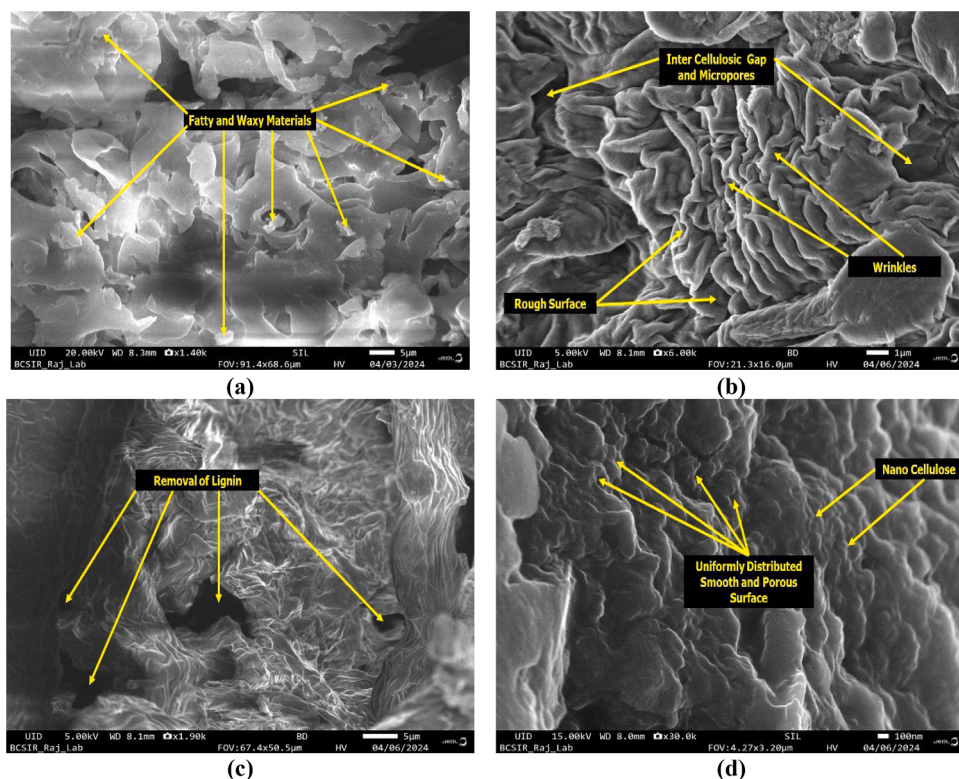


Fig. 5. FESEM micrographs of the subjected (a) raw fiber, (b) alkali treated fiber, (c) bleached fiber, and (d) maize cob derived CNC under the magnification range of 1,400x to 30,000x.

Fig. 5 (c), The FESEM micrograph of bleached fiber designates that there stands a sharp difference between raw, alkali treated, and bleached fiber. Due to the presence of hydroxyl and carboxyl group cellulose fiber are negatively charged. Although in raw fiber hydroxyl and carboxyl groups were covered by lignin after bleaching process bundle of lignin successfully removed which is clearly marked in **Fig. 5 (d)**, the FESEM micrograph of bleached fiber. Comparison of the previous two FESEM micrograph of raw and alkali treated fiber with the microgram of bleached fiber prescribes that surface of bleached fiber became smooth which is undoubtedly as a result of successful removal of lignin, hemicellulose, and impurities. **Fig. 6** dictates the average particle size of isolated CNC was at a range of around 1–100 nm which was calculated by the help of Origin lab and ImageJ software using the FESEM micrograph of maize cob CNC. Furthermore, there was originated a lot of crystalline structure of cellulose which were attributed due

to successful acid hydrolysis. Additionally, there was appeared lots of honey comb structures which indicates that the CNC would provide better capacity for reinforcement.

4.3. EDX analysis

EDX analysis result of raw fiber of maize cob at **Table 3 & Fig. 7 (a)** dictated the presence of 37.43% C, 61.03% O, 1.54% K. According to the literature review main constituents of lignocellulosic fibers are alpha cellulose, hemicellulose, lignin, etc. which are consist of carbon, hydrogen, and oxygen. That's why presence of oxygen and carbon molecules were detected during the elemental analysis. Although there was presence of huge amount of hydrogen molecules in the raw lignocellulosic fiber of maize cob but EDX analysis couldn't detect that because EDX can't detect small sized molecules like H, He, Li, etc. due to the lack of electrons in their outermost shell ([Rahman, 2024](#); [Rahman et al., 2024c](#); [Hossain et al., 2024](#)). Additionally, presence of K molecules in raw fiber since plants take different minerals from soil as macronutrient. Presence of 37.12% C, 58.26% O, 3.31% Ca, 1.31% Mg was noticed in EDX analysis, **Table 3 & Fig. 7 (b)** of alkali treated fiber. In alkali treated fiber composition of carbon and oxygen decreased compared to raw fiber which is due to the removal of hemicellulose (consist of carbon, oxygen, hydrogen). Additionally, presence of Ca, Mg

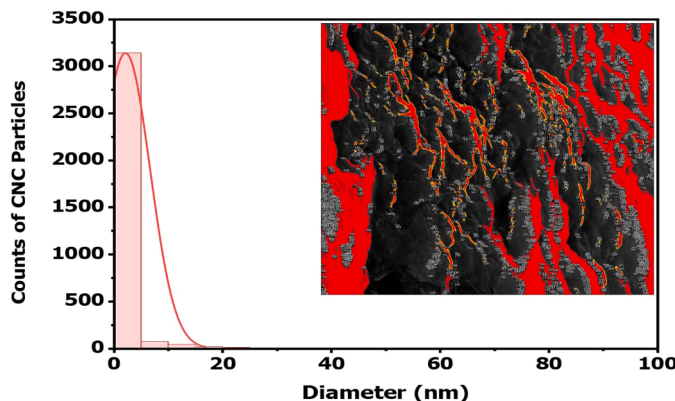


Fig. 6. Maize cob derived CNC particles size distribution profile (Histogram) in 1 to 100 nm range, determined from the FESEM micrograph of maize cob CNC (with the help of ImageJ and Origin lab software).

Table 3

Elemental composition of raw, alkali treated, bleached fiber, and maize cob CNC found in EDX analysis.

Sample	Elemental Composition (%)						
	C	O	Si	K	Ca	Mg	S
Raw fiber	37.43	61.03	-	1.54	-	-	-
Alkali treated fiber	37.12	58.26	-	-	3.31	1.31	-
Bleached fiber	41.85	58.15	-	-	-	-	-
CNC	39.55	42.08	3.81	-	2.78	-	11.78

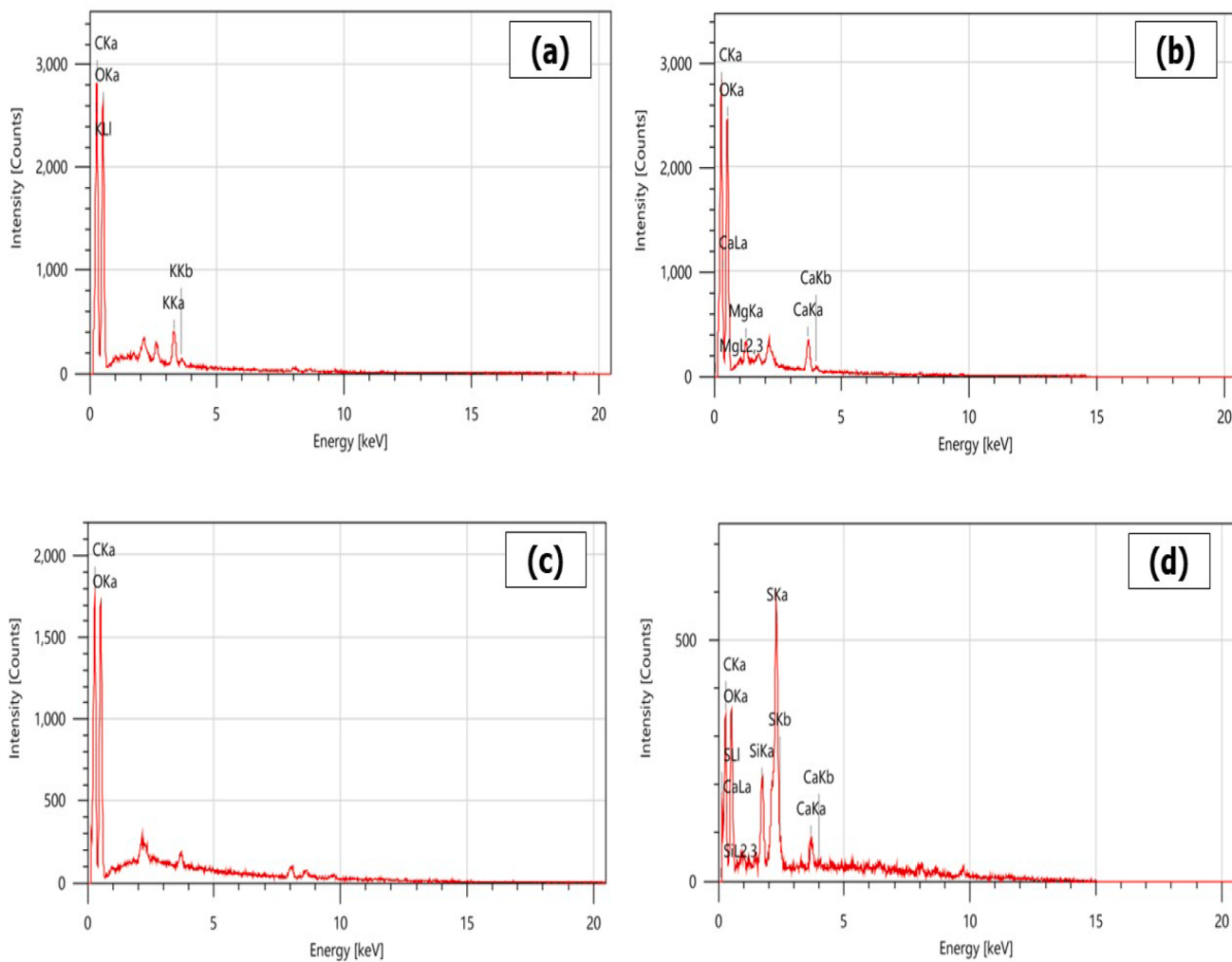


Fig. 7. Resultant images of EDX analysis (carried out for elemental analysis) in case of the (a) raw fiber, (b) alkali treated fiber, (c) bleached fiber, and (d) maize cob derived CNC.

may be because of impurities of NaOH which was used during alkali treatment. Bleached fiber, Fig. 7 (c) dictated the presence of 41.85% C, 58.15% O. Sample analysis of CNC, Fig. 7 (d) indicated that the composition of C, O, Si, Ca, S in the isolated CNC was 39.55%, 42.08%, 3.81%, 2.78%, 11.78% respectively. Presence of Si in the CNC which may be came from air. Further arrival of Ca may be due to chemical impurities of acid which was used for hydrolysis. Furthermore, existence of S could be because of chemical modification of sulfuric acid.

4.4. Thermal analysis (TGA/DTG/DTA)

Mass loss of raw maize cob fiber, bleached fiber, alkali treated fiber, and maize cob CNC in the temperature range of 0 °C to 100 °C was about 10% during thermal analysis which was basically evaporative loss, Fig. 8 (a). Curves are horizontal in the temperature range of 100 °C to 250 °C which dictates that during thermal analysis moisture was released at a constant rate of 10% at that temperature range. In the temperature range of 250 °C to 340 °C about 65% and 30% moisture was released from the alkali treated fiber and CNC specimen respectively whereas in case of raw and bleached fiber respectively about 55% and 60% moisture was released in the temperature range of 250 °C to 375 °C according to this comparison it can be said that CNC is better heat stable. About 10% mass loss was noticed in case of raw and bleached fiber in the temperature range of 375 °C to 600 °C, Fig. 8 (a). On the other hand, in alkali treated fiber loss of mass about 14% in the temperature range of

350 °C to 600 °C. But in CNC about 12% moisture loss observed due to low thermal decomposition during TG analysis (residual mass of CNC was around 40%) in the temperature range of 325 °C to 600 °C, Fig. 8 (a) which indicates that maize cob CNC is much more thermally stable than other fibers i.e., raw maize cob fiber, bleached fiber, alkali treated fiber. Degradation of cellulose, which may include hydroxyl group rupture, β-1,4 glycoside linkage breakdown, hemicellulose depolymerization, and dehydration, was the reason for the weight loss of different specimen (Rahman and Maniruzzaman, 2019; Rahman et al., 2024e). Rate of mass loss of CNC, raw fiber, bleached fiber, and alkali treated fiber at 75 °C was 95 µg/min, 200 µg/min, 550 µg/min, 425 µg/min respectively, Fig. 8 (b). In the temperature range of 200 °C to 400 °C mass loss rate was 570 µg/min, 5100 µg/min, 690 µg/min, 3600 µg/min in case of CNC, alkali treated fiber, raw fiber, and bleached fiber respectively, Fig. 8 (b). Further, mass loss with respect to time in the temperature range of 400 °C to 600 °C for CNC, raw fiber, bleached fiber, and alkali treated fiber was 30 µg/min, 115 µg/min, 300 µg/min, 280 µg/min respectively, Fig. 8 (b). According to the DTG analysis of all specimen it can be claimed that CNC showed more thermal stability in various temperature compared to other samples. (Kiziltas et al., 2016; Rahman, 2024; Zor et al., 2023). Heat loss due to endothermic reaction appeared at the temperature of around 75 °C and 120 °C in case of raw fiber, CNC and alkali, bleached fiber respectively which dictated in the DTA curve, Fig. 8 (c).. Some exothermic reaction occurred at 260 °C, 250 °C, 270 °C, 230 °C, 325 °C in CNC, alkali treated fiber, bleached fiber, raw fiber,

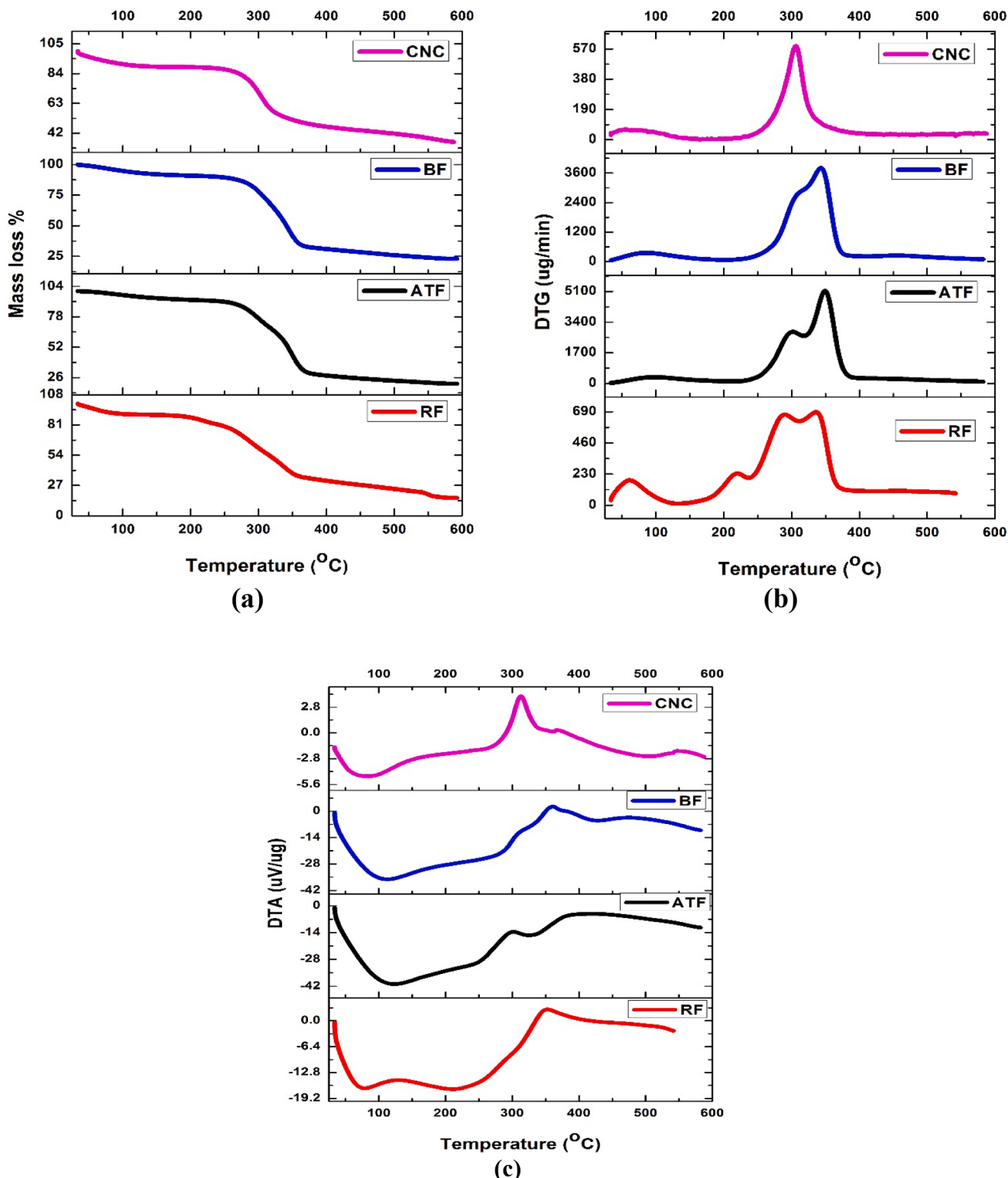


Fig. 8. Overall thermal analysis, (a) TGA, (b) DTG, and (c) DTA of the subjected specimen (raw fiber, alkali treated fiber, bleached fiber, and maize derived cob CNC) up to 600 °C.

alkali treated fiber respectively that ensured by the sharp peak at their respected temperature Fig. 8 (c). Furthermore, at 350 °C 330 °C, 340 °C & 430 °C, 400 °C, a few exothermic reactions taken place in case of CNC, alkali treated fiber, bleached fiber, and raw fiber respectively. CNC sample again undergone an exothermic reaction at 500 °C (Rahman &

Maniruzzaman, 2021; Hossain et al., 2024). As per thermal analysis (TGA, DTG, DTA) it could be professed that the isolated CNC is thermally more stable compared to raw maize cob fiber, bleached fiber, and alkali treated fiber.

4.5. XRD analysis

XRD patterns of raw maize cob fiber, bleached fiber, alkali treated fiber, and maize cob CNC shown in the Fig. 9. Peaks in XRD data at around $2\theta = 12.6^\circ$ (plane 001), 21° (plane 110), 22.5° (plane 002), 29° (plane 111), 30° (plane 220), and 35° (plane 004) (Fig. 9.) demonstrates that extracted nanocellulose crystals take on a crystalline structural form. The crystallinity index (C_{rI}) of all the analyzed specimen was calculated by using the Eq. (1) and is tabulated (Table 4.). The hemicellulose and lignin contents were eliminated to some extent in the amorphous zone during the alkali process, which caused the crystallinity index to rise gradually (N.H. Abdul-Rahman et al., 2017; Hassan et al., 2024; Rahman et al., 2024c & 2024d). The bundle of lignin was removed during the bleaching process, which caused the crystalline spheres to reorganize. The reduction of the amorphous area in cellulose by hydrolysis processes is reflected by the high crystallinity index of nanocellulose. The amorphous area can disintegrate with acid hydrolysis, making it less stable than the crystalline sections. Acid hydrolysis at a high concentration removes the amorphous portion of cellulose as well as breaks down the crystalline portion of cellulose. Hydronium ions migrate into cellulose amorphous areas during the acid hydrolysis process, assigning glycosidic linkages of hydrolytic cleavage that finally issues unique crystallites. Due to the increasing of crystallinity of fibers of maize cob, rigidity, toughness, strength was also increased. In raw fiber, the proportion of crystallinity index was $38.09 \pm 0.01\%$ and in extracted CNC (with a JCPDS-ICDD card number (00–056–1718)), this value risen to $84.63 \pm 0.03\%$, Table 5 and a comparative study of crystallinity index of the CNC collect from different sources (see Table 6) (Nagalakshmaiah et al., 2019; Marett et al., 2017; Thakur et al., 2020; Kumar et al., 2013). Amorphous nano compounds such as hemicellulose and lignin were successfully eliminated by using alkali treatment, bleaching, and acid hydrolysis as a result CNC provided higher crystallinity index value (Aisyah et al., 2020; Guo et al., 2020).

4.6. Particles size and zeta potential analysis

According to the DLS analysis the nanocellulose particles belongs to the range of 100–200 nm, Fig. 10 (a) while Fig. 10 (b) have shown the multiple bar chart for better understanding the average particle size of the newly produced CNCs. Whereas most of the CNC particles (about

Table 4

TGA, DTA, and DTG thermal analysis, mass loss, reaction mechanism, and degradation rate of various chemically treated fibers (raw fiber, alkali treated fiber, bleached fiber, and maize cob CNC).

Parameters	Raw fiber (% at $^{\circ}\text{C}$)	Alkali treated fiber (% at $^{\circ}\text{C}$)	Bleached fiber (% at $^{\circ}\text{C}$)	CNC (% at $^{\circ}\text{C}$)
Initial loss	15 at 75	12.5 at 95	13.5 at 100	16 at 100
Maximum loss	86 at 600	82 at 600	78 at 600	60 at 600
50% degradation ($^{\circ}\text{C}$)	300	320	330	310
Highest degradation ($^{\circ}\text{C}$)	599	598	595	592
Residue at 600 $^{\circ}\text{C}$	13	17	23	40
Endothermic peak at $^{\circ}\text{C}$	75, 220, 420	120, 250, 330	120, 280, 330, 430	75, 270, 350, 500
Maximum rate of mass loss ($\mu\text{g}/\text{min}$)	690	5100	3600	570

Table 5

Crystallinity index of the subjected raw fiber, alkali treated fiber, bleached fiber, and CNC of maize cob according to the XRD analysis of this current work.

Name of the samples	Crystallinity Index (C_{rI} %) value
Raw fiber	38.09 ± 0.01
Alkali treated fiber	45.17 ± 0.05
Bleached fiber	72.39 ± 0.07
CNC	84.63 ± 0.03

The data are shown in Table 5 as mean \pm standard deviation (SD), and there were three trials ($n = 3$). It has been statistically examined using analysis of variance (ANOVA) in order to determine if the sample's characteristics differ substantially at the 5% ($p < 0.05$) level.

60%) have possessed their hydrodynamic radius around 160 to 180 nm, additionally about 22% particles have possessed below 150 nm and rest of the particles have shown their size below 200nm but higher than 180 nm respectively. Since in DLS analysis the particles size was observed in

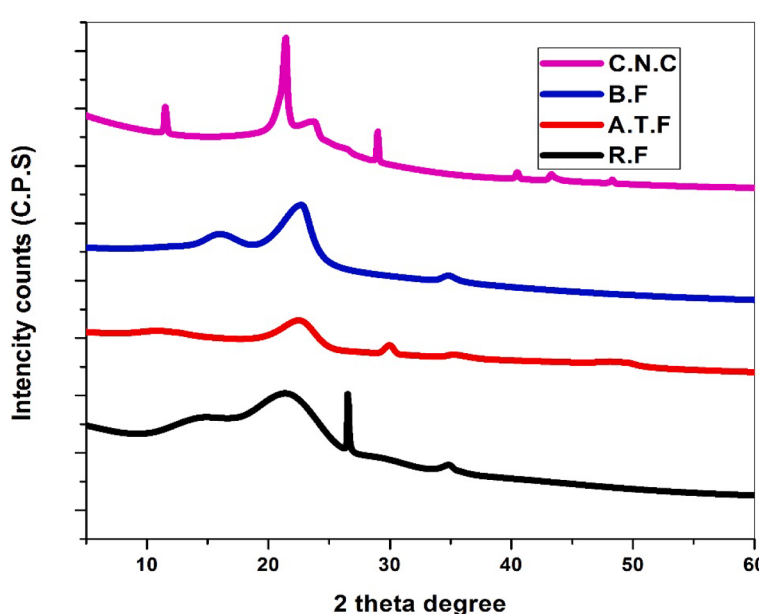


Fig. 9. Comparative XRD analysis of the subjected raw fiber, alkali treated fiber, bleached fiber, and maize cob derived CNC in the range of 5° to 60° (2θ) with respective crystalline planes (while CPS stand for counts per second).

Table 6

Comparative study of crystallinity index of the CNC collect from different sources and maize cob according to the XRD analysis.

Source	Crystallinity Index (C _r I)Value (%)	Reference
Garlic straw	68.80%	(Nagalakshmaiah et al., 2019)
Chili leftover	78.50%	
Groundnut shells	74.00%	
Pistachio shells	66.00%	(Marett et al., 2017)
Rice straw	76.00%	(Thakur et al., 2020)
Sugarcane bagasse	72.50%	(Kumar et al., 2013)
Keya leaf	61.31%	(Hossain et al., 2024)
Okra stalks	86.09%	(Rahman et al., 2024b)
Maize cob	84.63 ± 0.03%	This study

nano range it is confirmed that the nanocellulose was isolated successfully. The zeta potential value of extracted maize cob CNC was found around -7.09mV, Fig. 10 (c) which dictates that lots of negative charge were present on the surface of nanocellulose. Notably, inside the lattice

of the subjected CNC solids, both the positive as well as negative charges are recompensed because of the electro-neutrality of the considered stable compounds like nanocellulose. Once reaching the peripheral surface of the newly produced CNCs, the rhythm could be destroyed while some charges persist unpaid, hence the electro-neutrality should have been lost then the surface of the subjected crystalline solids are charged (Serrano-Lotina et al., 2023). However, the sign as well as the magnitude of the newly appeared charges that are belong to the surface of the CNCs could be responsible to govern the endorsement of the ionic species from the existing solutions as well as the physical properties of distributions. Conversely, it is well known to all that with the increasing of the value of negative surface charge/zeta potential of the subjected CNC particles the stability of those particles have also shown an increasing tendency this could be happened due to the electrostatic repulsion forces among the similarly charged CNCs particles (Hossain et al., 2024; Selvamani et al., 2019; Rahman et al., 2024b).

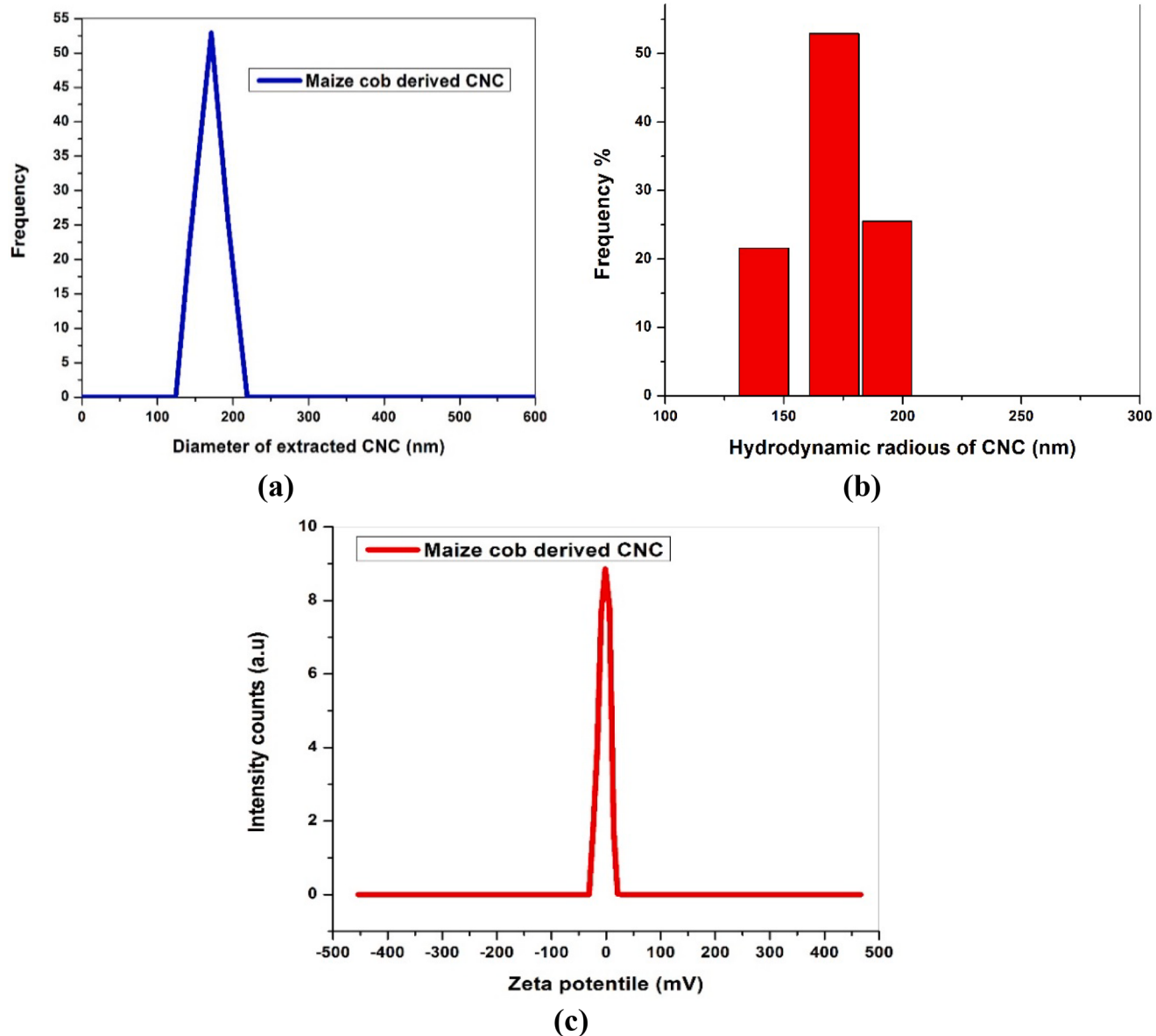


Fig. 10. (a) Particles size distribution (within 0 to 600 nm range) according to the DLS method, (b) Multiple bar chart addressing the different size of the CNC particles, and (c) Zeta potential (within -500 mV to +500mV range) of the maize cob derived CNC (while a.u stand for arithmetic unit).

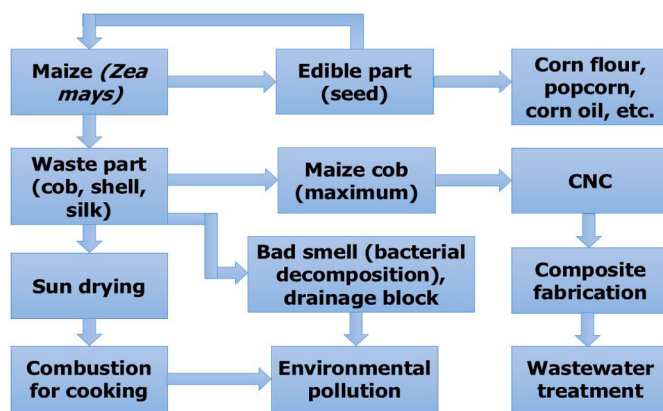


Fig. 11. Life cycle analysis of *Z. mays* as well as comparison of the environmental and economic impact focusing on its major waste called maize cob, a source of CNC.

5. Conclusion

In this study, useless lignocellulosic agro waste (maize cob) was utilized to extract potentially valuable CNC via several chemical modification steps such as scouring, alkali treatment, bleaching, and acid hydrolysis (H_2SO_4). Characterization of the raw maize cob fiber, bleached fiber, alkali treated, and extracted maize cob CNC were carried out by conducting a quite number of state-of-the-art equipment's like FTIR-ATR, FESEM, EDX, TG (TGA/DTG/DTA), DLS, Zeta potential analysis, and XRD analysis. Effective modification was noticed in the absorption pattern of comparative FTIR-ATR spectrum of individual fibers. Each step of modification exposes new face look in the FESEM micrographs (2D honeycomb like peripheral surface microstructure) and elemental composition also altered as observed in EDX analysis. Higher residual mass of CNC (around 40%) as observed in TGA analysis dictated that the isolated CNC was thermally more stable compared to all other specimens such as raw, alkali treated, and bleached maize cob fibers. Isolated CNC given lowest rate of mass loss of $40 \mu\text{g}/\text{min}$ which indicates that extracted CNC was highly thermal stable due to its purity. Analyzing the particles size it was found that the average particles size of the newly produced CNC was around 100 nm in sized. The highest value of crystallinity index was found at approximately around $84.63 \pm 0.03\%$ in case of the subjected CNC according to the XRD analysis. Due to these outstanding properties along with negative surface charge the newly produced CNC could be promising to fabricate a very much strength multifunctional biopolymeric nanocomposites that should have a very good agreement with sustainable environmental development. Hence, they would be beneficially used in various sectors including bulky industrial, engineering, as well as biomedical fields in order to maintain the climate and biodiversity.

Funding

The authors extend their appreciation to the Ministry of Science and Technology (MOST), the People's Republic of Bangladesh, and the Bangladesh Council of Scientific and Industrial Research (BCSIR), for their joint funding to conduct this current work through Research and Development Project under grant number of (G.O. 39.00.0000.012.02.009.23.159 and G.O. 39.02.0000.011.14.169.2023/877).

CRediT authorship contribution statement

Shamim Dewan: Writing – original draft, Software, Methodology, Conceptualization. **Md. Mahmudur Rahman:** Writing – review & editing, Writing – original draft, Visualization, Validation, Supervision,

Software, Resources, Project administration, Methodology, Investigation, Funding acquisition, Formal analysis, Data curation, Conceptualization. **Md. Ismail Hossain:** Validation, Software, Investigation. **Bijoy Chandra Ghos:** Investigation, Formal analysis, Data curation. **M Mohinur Rahman Rabby:** Software, Resources, Methodology. **Md. Abdul Gafur:** Resources, Methodology. **Md. Al-Amin:** Software, Investigation. **Md. Ashraful Alam:** Software, Resources.

Declaration of competing interest

The authors declare that they have no known competing financial interests or personal relationships that could have appeared to influence the work reported in this paper.

Acknowledgment

All authors of this paper devoutly acknowledge the chairman of Bangladesh Council of Scientific and Industrial Research (BCSIR), as well as the Ministry of Science and Technology (MOST), People's Republic of Bangladesh for their financial support and for consenting us to conduct their highly sophisticated instruments for experimentation. Furthermore, I want to acknowledge my better-half Suriaya Naznin, lab attendant Md. Mofijul Islam and Mst. Ronjina Khatun for their cordial help and support during the experimental session and drafting.

References

- Abdul-Rahman, N.H., Chieng, B.W., Ibrahim, N.A., Abdul-Rahman, N., 2017. Extraction and characterization of cellulose nanocrystals from tea leaf waste fibers. *Polymers*. (Basel) 9, 588. <https://doi.org/10.3390/polym9110588>.
- Aisiyah, M.M., Masruri, M., Srihardyastuti, A., 2020. Crystallinity of nanocellulose isolated from the flower waste of pine tree (*Pinus merkusii*). In: IOP Conference Series: Materials Science and Engineering, 833. <https://doi.org/10.1088/1757-899X/833/1/012003>.
- Akinjokun, A.I., Petrik, L.F., Ogunfowokan, A.O., Ajao, J., Ojumu, T.V., 2021. Isolation and characterization of nanocrystalline cellulose from cocoa pod husk (CPH) biomass wastes. *Heliyon*. 7. <https://doi.org/10.1016/j.heliyon.2021.e06680>.
- Ali, M., 2016. Microstructure, thermal analysis and acoustic characteristics of calotropis procera (apple of sodom) Fibers. *J. Natural Fibers* 13, 343–352. <https://doi.org/10.1080/15440478.2015.1029198>.
- Alojaly, H., Benyounis, K.Y., 2022. Packaging with plastics and polymeric materials. encyclopedia of materials: plastics and polymers. 3, 485–501. <https://doi.org/10.1016/B978-0-12-820352-1.00025-0>.
- Babaremu, K., Oladijo, O.P., Akinlabi, E., 2023. Biopolymers: a suitable replacement for plastics in product packaging. *Adv. Indust. Eng. Polymer Res.* 6, 333–340. <https://doi.org/10.1016/J.AIEPR.2023.01.001>.
- Bano, S., Negi, Y.S., 2017. Studies on cellulose nanocrystals isolated from groundnut shells. *Carbohydrate Polymers* 157, 1041–1049. <https://doi.org/10.1016/J.CARBPOL.2016.10.069>.
- Benini, K.C.C., de, C., Voorwald, H.J.C., Cioffi, M.O.H., Rezende, M.C., Arantes, V., 2018. Preparation of nanocellulose from imperata brasiliensis grass using taguchi method. *Carbohydrate Polymers* 192, 337–346. <https://doi.org/10.1016/J.CARBPOL.2018.03.055>.
- Bhattacharjee, S., 2016. DLS and zeta potential - what they are and what they are not? *J. Controlled Release* 235, 337–351. <https://doi.org/10.1016/j.jconrel.2016.06.017>.
- Chaka, K.T., 2022. Extraction of cellulose nanocrystals from agricultural by-products: a review. *Green. Chem. Lett. Rev.* 15, 582–597. <https://doi.org/10.1080/17518253.2022.2121183>.
- Chen, X.Q., Pang, G.X., Shen, W.H., Tong, X., Jia, M.Y., 2019. Preparation and characterization of the ribbon-like cellulose nanocrystals by the cellulase enzymolysis of cotton pulp fibers. *Carbohydrate Polymers*. 207, 713–719. <https://doi.org/10.1016/J.CARBPOL.2018.12.042>.
- Cheran, E., Rahale, C.S., Lakshmanan, A., Subramanian, P., Raja, K., Divyabharathi, P., 2022. Synthesis and characterization of a novel maize cob based nanocellulose. *Int. J. Plant Soil. Sci.* 34, 678–687. <https://doi.org/10.9734/ijpps/2022/v34i2131318>.
- Corrêa, A.C., de Teixeira, E.M., Pessan, L.A., Mattoso, L.H.C., 2010. Cellulose nanofibers from curaua fibers. *Cellulose* 17, 1183–1192. <https://doi.org/10.1007/s10570-010-9453-3>.
- Costa, L.A.S., Assis, D.J., Gomes, G.V.P., Silva, J.B.A., Fonsêca, A.F., Druzian, J.I., 2015. Extraction and characterization of nanocellulose from corn stover. *Mater. Today: Proc.* 2, 287–294. <https://doi.org/10.1016/j.matpr.2015.04.045>.
- Deepa, B., Abraham, E., Cherian, B.M., Bismarck, A., Blaker, J.J., Pothan, L.A., Leao, A. L., de Souza, S.F., Kottaisamy, M., 2011. Structure, morphology and thermal characteristics of banana nano fibers obtained by steam explosion. *Bioresour. Technol.* 102, 1988–1997. <https://doi.org/10.1016/J.BIOTECH.2010.09.030>.
- Dhali, K., Daver, F., Cass, P., Adhikari, B., 2021. Isolation and characterization of cellulose nanomaterials from jute bast fibers. *J. Environ. Chem. Eng.* 9, 106447. <https://doi.org/10.1016/J.JECE.2021.106447>.

- Du, H., Liu, W., Zhang, M., Si, C., Zhang, X., Li, B., 2019. Cellulose nanocrystals and cellulose nanofibrils based hydrogels for biomedical applications. *Carbohydrate Polymers*. 209, 130–144. <https://doi.org/10.1016/j.carbpol.2019.01.020>.
- El Messaoudi, N., Miyah, Y., Georgin, J., Wasilewska, M., Felisardo, R.J.A., Moukadiri, H., Manzar, M.S., Aryee, A.A., Knani, S., Rahman, M.M., 2024. Recent developments in the synthesis of tetraethylengenetamine-based nanocomposites to eliminate heavy metal pollutants from wastewater through adsorption. *Bioresour. Technol. Rep.* 28, 101982. <https://doi.org/10.1016/j.biteb.2024.101982>.
- Eubeler, J.P., Zok, S., Bernhard, M., Knepper, T.P., 2009. Environmental biodegradation of synthetic polymers I. test methodologies and procedures. *TrAC Trends Anal. Chem.* 28, 1057–1072. <https://doi.org/10.1016/j.TRAC.2009.06.007>.
- Guo, Y., Zhang, Y., Zheng, D., Li, M., Yue, J., 2020. Isolation and characterization of nanocellulose crystals via acid hydrolysis from agricultural waste-tea stalk. *Int. J. Biol. Macromol.* 163, 927–933. <https://doi.org/10.1016/j.ijbiomac.2020.07.009>.
- Hassan, M.M., Rahman, M.M., Ghos, B.C., Hossain, M.I., Amin, M.A., Zuhane, M.K.A., 2024. Extraction, and characterization of CNC from waste sugarcane leaf sheath as a reinforcement of multifunctional bio-nanocomposite material: a waste to wealth approach. *Carbon Trends* 17, 100400. <https://doi.org/10.1016/j.cartre.2024.100400>.
- Hayat, H., Mahmood, Q., Pervez, A., Bhatti, Z.A., Baig, S.A., 2015. Comparative decolorization of dyes in textile wastewater using biological and chemical treatment. *Separation Purification Technol.* 154, 149–153. <https://doi.org/10.1016/J.SEPPUR.2015.09.025>.
- Hossain, M.I., Rahman, M.M., Ghos, B.C., Gafur, M.A., Alam, M.A., Rabbi, M.A., 2024. Preparation and characterization of crystalline nanocellulose from keya (*Pandanus tectorius*) L. fiber as potential reinforcement in sustainable bionanocomposite: a waste to wealth scheme. *Carbohydrate Polymer Technol. Appl.* 8, 100600. <https://doi.org/10.1016/j.cartpa.2024.100600>.
- Kabir, M.S., Hossain, M.S., Mia, M., Islam, M.N., Rahman, M.M., Hoque, M.B., Chowdhury, A.M.S., 2018. Mechanical properties of gamma-irradiated natural fiber reinforced composites. *Nano Hybr. & Compos.* 23, 24–38. <https://doi.org/10.4028/www.scientific.net/nhc.23.24>.
- Kampeerapappun, P., 2015. Extraction and characterization of cellulose nanocrystals produced by acid hydrolysis from corn husk. *J. Metals, Mater. Minerals.* 25, 19–26. <https://doi.org/10.14456/jmmm.2015.3>.
- Karak, N., 2012. Vegetable oil-based polymer composites. *Vegetable Oil-Based Poly.* 247–270. <https://doi.org/10.1533/9780857097149.247>.
- Karimah, A., Ridho, M.R., Munawar, S.S., Adi, D.S., Ismail, Damayanti, R., Subiyanto, B., Fatriasari, W., Fudholi, A., 2021. A review on natural fibers for development of eco-friendly bio-composite: characteristics, and utilizations. *J. Mater. Res. Technol.* 13, 2442–2458. <https://doi.org/10.1016/j.jmrt.2021.06.014>.
- Kassab, Z., Abdellaoui, Y., Salim, M.H., Bouhfid, R., Qais, A.E.K., Achaby, M.E., 2020. Micro- and nano-celluloses derived from hemp stalks and their effect as polymer reinforcing materials. *Carbohydr. Polym.* 245, 116506. <https://doi.org/10.1016/j.carbpol.2020.116506>.
- Khan, M.N., Rehman, N., Sharif, A., Ahmed, E., Farooqi, Z.H., Din, M.I., 2020. Environmentally benign extraction of cellulose from dunichi fiber for nanocellulose fabrication. *Int. J. Biol. Macromol.* 153, 72–78. <https://doi.org/10.1016/J.IBJOMAC.2020.02.333>.
- Khatun, M.A., Sultana, S., Islam, Z., Kabir, M.S., Hossain, M.S., Nur, H.P., Chowdhury, A. M.S., 2023. Extraction of crystalline nanocellulose (CNC) from date palm mat fibers and its application in the production of nanocomposites with polyvinyl alcohol and polyvinylpyrrolidone blended films. *Results. Eng.* 17, 101031. <https://doi.org/10.1016/J.RINENG.2023.101031>.
- Kiziltas, E.E., Yang, H.S., Kiziltas, A., Boran, S., Ozen, E., Gardner, D.J., 2016. Thermal analysis of polyamide 6 composites filled by natural fiber blend. *BioResources* 11, 4758–4769. <https://doi.org/10.1537/biores.12.2.4758-4769>.
- Komuraiah, A., Kumar, S.N., Prasad, D.B., 2014. Chemical composition of natural fibers and its influence on THEIR mechanical properties. *Mech. Composite Mater.* 50 (3). <https://doi.org/10.1007/s11029-014-9422-2>.
- Kondor, A., Santmarti, A., Mautner, A., Williams, D., Bismarck, A., Lee, K.Y., 2021. On the BET Surface area of nanocellulose determined using volumetric, gravimetric and chromatographic adsorption methods. *Front. Chem. Eng.* 3. <https://doi.org/10.3389/fceng.2021.738995>.
- Kumar, A., Negi, Y.S., Choudhary, V., Bhardwaj, N.K., 2013. Characterization of cellulose nanocrystals produced by acid-hydrolysis from sugarcane bagasse as agro-waste. *J. Mater. Phys. Chem.* 2, 1–8. <https://doi.org/10.12691/jmpc-2-1-1>.
- Kusmono, Listyanda, R.F., Wildan, M.W., Ilman, M.N., 2020. Preparation and characterization of cellulose nanocrystal extracted from ramie fibers by sulfuric acid hydrolysis. *Helixon* 6 (11), e05486, 10.1016%2Fj.helixon.2020.e05486.
- Leão, R.M., Miléo, P.C., Maia, J.M.L.L., Luz, S.M., 2017. Environmental and technical feasibility of cellulose nanocrystal manufacturing from sugarcane bagasse. *Carbohydr. Polym.* 175, 518–529. <https://doi.org/10.1016/J.CARBPOL.2017.07.087>.
- Li, B., Xu, W., Kronlund, D., Määttänen, A., Liu, J., Smått, J.H., Peltonen, J., Willföör, S., Mu, X., Xu, C., 2015. Cellulose nanocrystals prepared via formic acid hydrolysis followed by TEMPO-mediated oxidation. *Carbohydr. Polym.* 133, 605–612. <https://doi.org/10.1016/J.CARBPOL.2015.07.033>.
- Li, H., Shi, H., He, Y., Fei, X., Peng, L., 2020. Preparation and characterization of carboxymethyl cellulose-based composite films reinforced by cellulose nanocrystals derived from pea hull waste for food packaging applications. *Int. J. Biol. Macromol.* 164, 4104–4112. <https://doi.org/10.1016/J.IJBIMAC.2020.09.010>.
- Li, R., Fei, J., Cai, Y., Li, Y., Feng, J., Yao, J., 2009. Cellulose whiskers extracted from mulberry: A novel biomass production. *Carbohydr. Polym.* 76, 94–99. <https://doi.org/10.1016/J.CARBPOL.2008.09.034>.
- Lin, N., Dufresne, A., 2014. Nanocellulose in biomedicine: current status and future prospect. *Eur. Polym. J.* 59, 302–325. <https://doi.org/10.1016/j.europolymj.2014.07.025>.
- Liu, C., Li, B., Du, H., Lv, D., Zhang, Y., Yu, G., Mu, X., Peng, H., 2016. Properties of nanocellulose isolated from corn cob residue using sulfuric acid, formic acid, oxidative and mechanical methods. *Carbohydr. Polym.* 151, 716–724. <https://doi.org/10.1016/j.carbpol.2016.06.025>.
- Loganathan, S., Valapa, R.B., Mishra, R.K., Pugazhenthi, G., Thomas, S., 2017. Thermogravimetric analysis for characterization of nanomaterials. *Thermal Rheol. Measurement Techniques for Nanomater. Character.* 3, 67–108. <https://doi.org/10.1016/B978-0-323-46139-9.00004-9>.
- Loya, R.J., Lerma, M., Torresdey, G.L.J., 2024. Dynamic light scattering and its application to control nanoparticle aggregation in colloidal systems: a review. *Micromachines. (Basel)* 15. <https://doi.org/10.3390/mi15010024>.
- Lu, P., Hsieh, Y.L., 2012. Preparation and characterization of cellulose nanocrystals from rice straw. *Carbohydr. Polym.* 87, 564–573. <https://doi.org/10.1016/j.carbpol.2011.08.022>.
- Mao, Y., Liu, K., Zhan, C., Geng, L., Chu, B., Hsiao, B.S., 2017. Characterization of nanocellulose using small-angle neutron, x-ray, and dynamic light scattering techniques. *J. Phys. Chem. B* 121, 1340–1351. <https://doi.org/10.1021/acs.jpcb.6b11425>.
- Marett, J., Aning, A., Foster, E.J., 2017. The isolation of cellulose nanocrystals from pistachio shells via acid hydrolysis. *Ind. Crops. Prod.* 109, 869–874. <https://doi.org/10.1016/j.indcrop.2017.09.039>.
- Moros, M., Tino, A., Tortiglione, C., Moragas, G.L., Laromaine, A., 2019. Invertebrate models for hyperthermia: what we learned from caenorhabditis elegans and hydra vulgaris. *Nanomat. Magnetic Opt. Hyperthermia Appl.* 229–264. <https://doi.org/10.1016/B978-0-12-813928-8.00009-0>.
- Muthu, S.S., Gardetti, M.A., 2020. Sustainability in the Textile and Apparel Industries. *Sustainable Textiles: Production, Processing, Manufacturing & Chemistry.* <https://doi.org/10.1007/978-3-030-38541-5>.
- Nagalakshmaiah, M., Rajinipriya, M., Afrin, S., Ansari, M.A., Asad, M., Karim, Z., 2019. Cellulose nanocrystals-based nanocomposites. *Bio-based Polymers Nanocomposites* 49–65. https://doi.org/10.1007/978-3-030-05825-8_349.
- Nasrollahzadeh, M., Atarov, M., Sajjadi, M., Sajadi, S.M., Issaabadi, Z., 2019. Plant-Mediated green synthesis of nanostructures: mechanisms, characterization, and applications. *Interface Sci. Technol.* 28, 199–322. <https://doi.org/10.1016/B978-0-12-813586-0-00006-7>.
- Noreen, S., Tahira, M., Ghamkhar, M., Hafiz, I., Bhatti, H.N., Nadeem, R., Murtaza, M.A., Yaseen, M., Sheikh, A.A., Naseem, Z., Younas, F., 2021. Treatment of textile wastewater containing acid dye using novel polymeric graphene oxide nanocomposites (GO/PAN, GO/PPy, GO/PSty). *J. Mater. Res. Technol.* 14, 25–35. <https://doi.org/10.1016/J.JMRT.2021.06.007>.
- Orasugh, J.T., Ghosh, S.K., Chattopadhyay, D., 2020. Nanofiber-reinforced biocomposites. *Fiber-Reinforced Nanocomposites: Fundamentals and Applications.* 199–233. <https://doi.org/10.1016/B978-0-12-819904-6.00010-4>.
- Patel, A., Paliwal, H., Sawant, K., Prajapati, B.G., 2024. Micro and nanoemulsion as drug carriers in Alzheimer's disease. *Alzheimer's Disease Adv. Drug Delivery Strategies* 319–345. <https://doi.org/10.1016/B978-0-443-13205-6.00013-3>.
- Pereira, P.H.F., Waldron, K.W., Wilson, D.R., Cunha, A.P., Brito, E.S.de, Rodrigues, T.H. S., Rosa, M.F., Azeredo, H.M.C., 2017. Wheat straw hemicelluloses added with cellulose nanocrystals and citric acid. effect on film physical properties. *Carbohydr. Polym.* 164, 317–324. <https://doi.org/10.1016/J.CARBOL.2017.02.019>.
- Perera, K.T.G.K., 2014. A study on the Impacts of corn cultivation (*Zea mays* (L.) family-pooaceae) on the properties of soil. *Int. J. Sci. Res. Publ.* 4 :17589719.
- Poornachandhra, C., Jayabalakrishnan, R.M., Balasubramanian, G., Lakshmanan, A., Selvakumar, S., Maheswari, M., John, J.E., 2023. Coconut husk fiber: a low-cost bioresource for the synthesis of high-value nanocellulose. *Biointerface Res. Appl. Chem.* 13. <https://doi.org/10.33263/BRIC136.504>.
- Prado, K.S., Spinacé, M.A.S., 2019. Isolation and characterization of cellulose nanocrystals from pineapple crown waste and their potential uses. *Int. J. Biol. Macromol.* 122, 410–416. <https://doi.org/10.1016/J.IJBIMAC.2018.10.187>.
- Raghuvanshi, V.S., Garnier, G., 2024. Nanoparticle decorated cellulose nanocrystals (CNC) composites for energy, catalysis, and biomedical applications. *Adv. Funct. Mater.*, 2412869 <https://doi.org/10.1002/adfm.202412869>.
- Rahman, M.M., 2024. Waste biomass derived chitosan-natural clay based bionanocomposites fabrication and their potential application on wastewater purification by continuous adsorption: A critical review. *S. Afr. J. Chem. Eng.* 48, 214–236. <https://doi.org/10.1016/j.sajce.2024.02.006>.
- Rahman, M.M., Maniruzzaman, M., 2024. Environmentally friendly strength-bio-composite preparation by grafting of HEMA onto shrimp chitosan without destroying original microstructure to enrich their physicochemical, thermomechanical, and morphological properties. *S. Afr. J. Chem. Eng.* 47, 300–311. <https://doi.org/10.1016/j.sajce.2023.12.005>.
- Rahman, M.M., Shaikh, M.A.A., Yeasmin, M.S., Gafur, M.A., Hossain, M.I., Alam, M.A., Khan, M.S., Paul, T., Quddus, M.S., 2024a. Simultaneous removal of Ni²⁺ and Congo red from wastewater by crystalline nanocellulose - Modified coal bionanocomposites: Continuous adsorption study with mathematical modeling. *Groundwater for Sustainable Development* 26, 101244. <https://doi.org/10.1016/j.gsd.2024.101244>.
- Rahman, M.M., Hossain, M.I., Hassan, M.M., Ghos, B.C., Rahman, M.S., Gafur, M.A., Alam, M.A., Zuhane, M.K.A., 2024b. Cellulose nanocrystal (CNC) from okra plant (*Abelmoschus esculentus* L.) stalks as a reinforcement in bionanocomposite fabrication: Extraction, processing, and characterization study. *Carbohydrate Polymer Technol. Appl.*, 100581 <https://doi.org/10.1016/j.cartpa.2024.100581>.

- Rahman, M.M., Maniruzzaman, M., Zaman, M.N., 2024c. Fabrication and characterization of environmentally friendly biopolymeric nanocomposite films from cellulose nanocrystal of banana M. Oranta (Sagar kala) tree rachis fibers and poly lactic acid: A new route. *S. Afr. J. Chem. Eng.* 50, 451–465. <https://doi.org/10.1016/j.sajce.2024.10.002>.
- Rahman, M.M., Hossain, M.I., Ghos, B.C., Gafur, M.A., Alam, M.A., Uddin, M.J., Yeasmin, M.S., Hasan, M., Chowdhury, T.A., Rana, G.M.M., Karmakar, A., Barmon, J., 2024d. Fabrication of CNC-AC Bionanosorbents from the Residual Mass of Magnolia Champaca L. Bark after Methanol Extraction for Wastewater treatment: Continuous column Adsorption Study. *Environmental Nanotechnology, Monitoring & Management*, 101015. <https://doi.org/10.1016/j.enmm.2024.101015>.
- Rahman, M.M., Hosen Pk, M.E., Waliullah, M., Hossain, M.I., Maniruzzaman, M., Ghos, B.C., 2024e. Production of cellulose nanocrystals from the waste banana (M. Oranta) tree rachis fiber as a reinforcement to fabricate useful bionanocomposite. *Carbohydrate Polymer Technol. Appl.* 8, 100607. <https://doi.org/10.1016/j.carpata.2024.100607>.
- Rahman, M.M., Maniruzzaman, M., Gafur, M.A., Al-Ahmari, K.M., Shawabkeh, A., Alsharif, A., Naznin, S., Al-Otaibi, J.S., 2024f. Fabrication of chitosan coated bentonite clay multifunctional nanosorbents from waste biomass for the effective elimination of hazardous pollutants from waterbodies: A fixed bed biosorption, mechanism, and mathematical model study. *International Journal of Biological Macromolecules* 282 (6), 137439. <https://doi.org/10.1016/j.ijbiomac.2024.137439>.
- Rahman, M.M., Maniruzzaman, M., Saha, R.K., 2024g. A green route of antibacterial films production from shrimp (*Penaeus monodon*) shell waste biomass derived chitosan: Physicochemical, thermomechanical, morphological and antimicrobial activity analysis. *South African Journal of Chemical Engineering*. <https://doi.org/10.1016/j.sajce.2024.11.005>.
- Rahman, M.M., Yeasmin, M.S., Uddin, M.J., Hasan, M., Shaikh, M.A.A., Rahman, M.S., Maniruzzaman, M., 2023a. Simultaneous abatement of Ni²⁺ and Cu²⁺ effectually from industrial wastewater by a low cost natural clay-chitosan nanocomposite filter: Synthesis, characterization and fixed bed column adsorption study. *Environ. Nanotechnol. Monit. Manage* 20, 100797. <https://doi.org/10.1016/j.enmm.2023.100797>.
- Rahman, M.M., Islam, M.M., Maniruzzaman, M., 2023b. Preparation and characterization of biocomposite from modified α-cellulose of Agave cantala leaf fiber by graft copolymerization with 2-hydroxy ethyl methacrylate. *Carbohydrate Polymer Technol. Appl.* 6 (701), 100354. <https://doi.org/10.1016/j.carpata.2023.100354>.
- Rahman, M.M., Maniruzzaman, M., Yeasmin, M.S., 2023c. A state-of-the-art review focusing on the significant techniques for naturally available fibers as reinforcement in sustainable bio-composites: extraction, processing, purification, modification, as well as characterization study. *Results. Eng.* 20. <https://doi.org/10.1016/j.rineng.2023.101511>.
- Rahman, M.M., Maniruzzaman, M., Yeasmin, M.S., Gafur, M.A., Shaikh, M.A.A., Alam, M.A., Uddin, M.J., Hasan, M., Bashera, M.Al, Chowdhury, T.A., Maitra, B., Naim, M.R., Rana, G.M.M., Saha, B.K., Quddus, M.S., 2023d. Adsorptive abatement of Pb²⁺ and crystal violet using chitosan-modified coal nanocomposites: A down flow column study. *Groundw. Sustain. Dev.* 23. <https://doi.org/10.1016/j.gsd.2023.101028>.
- Rahman, M.M., Maniruzzaman, M., Islam, R.M., Rahman, S.M., 2018a. Synthesis of nano-cellulose from okra fibre and FTIR as well as morphological studies on it. *Am. J. Polymer Sci. Technol.* 4, 42. <https://doi.org/10.11648/j.apst.20180402.11>.
- Rahman, M.M., Islam, M.R., Islam, M.R., Naznin, S., 2018b. Extraction and Characterization of Lipid from Pangus Fish (P. Pangasius) Available in Bangladesh by Solvent Extraction Method. *American Journal of Zoology* 1 (2), 28–34. <https://doi.org/10.11648/j.ajz.20180102.11>.
- Rahman, M.M., Maniruzzaman, M., 2019. Preparation of shrimp shell chitosan-clay-nanofilter for the purification of drinking water. *Int. J. Food Technol.* 2, 17–26. <https://doi.org/10.11648/j.jift.20180202.12>.
- Rahman, M.M., Maniruzzaman, M., 2021. Extraction of nanocellulose from banana rachis (agro waste) and preparation of nanocellulose-clay nanofilter for the industrial wastewater purification. *J. Bioremediat. Biodegrad.* 12 (485), 708. <https://doi.org/10.4172/2155-6199.1000485>.
- Rahman, O., Rahman, M.M., Maniruzzaman, M., 2022. Removal of dye and heavy metals from industrial wastewater by activated charcoal-banana rachis cellulose nanocrystal composite filter. *Int. J. Environ. Anal. Chem.* 104 (7), 1478–1496. <https://doi.org/10.1080/03067319.2022.2039647>.
- Rajanna, M., Shivashankar, L.M., Shivamurthy, O.H., Ramachandrappa, S.U., Betageri, V.S., Shivamallu, C., Shetty, R.H.L., Kumar, S., Amachawadi, R.G., Kollur, S.P., 2022. A facile synthesis of cellulose nanofibers from corn cob and rice straw by acid hydrolysis method. *Polymers (Basel)* 14, 4383. <https://doi.org/10.3390/polym14204383>.
- Rasheed, M., Jawaid, M., Parvez, B., Zuriyati, A., Khan, A., 2020. Morphological, chemical and thermal analysis of cellulose nanocrystals extracted from bamboo fibre. *Int. J. Biol. Macromol.* 160, 183–191. <https://doi.org/10.1016/j.ijbiomac.2020.05.170>.
- Ren, R.W., Chen, X.Q., Shen, W.H., 2022. Preparation and separation of pure spherical cellulose nanocrystals from microcrystalline cellulose by complex enzymatic hydrolysis. *Int. J. Biol. Macromol.* 202, 1–10. <https://doi.org/10.1016/j.ijbiomac.2022.01.009>.
- Rydz, J., 2024. Sustainability and environmental degradability of synthetic polymers. *Chem. Mol. Sci. Chem. Eng.* <https://doi.org/10.1016/B978-0-443-15742-4.00015-6>.
- Sartika, D., Firmansyah, A.P., Junais, I., Arnata, I.W., Fahma, F., Firmandi, A., 2023. High yield production of nanocrystalline cellulose from corn cob through a chemical-mechanical treatment under mild conditions. *Int. J. Biol. Macromol.* 240, 124327. <https://doi.org/10.1016/j.ijbiomac.2023.124327>.
- Selvamani, V., 2019. Chapter 15 - stability studies on nanomaterials used in drugs, in micro and nano technologies. *Charact. Biol. Nanomater. Drug Delivery* 425–444. <https://doi.org/10.1016/B978-0-12-814031-4.00015-5>.
- Sepevani, A.A., Evans, D.A.C., Annamalai, P.K., Martin, D.J., 2017. The use of cellulose nanocrystals to enhance the thermal insulation properties and sustainability of rigid polyurethane foam. *Ind. Crops. Prod.* 107, 114–121. <https://doi.org/10.1016/J.INDCROP.2017.05.039>.
- Serrano-Lotina, A., Portela, R., Baeza, P., Alcolea-Rodriguez, V., Villarroel, M., Ávila, P., 2023. Zeta potential as a tool for functional materials development. *Catal. Today* 423, 113862. <https://doi.org/10.1016/j.cattod.2022.08.004>.
- Sheikh, S.M., Rahman, M.M., Rahman, S.M., Yildirim, K., Maniruzzaman, M., 2023. Fabrication of nano composite membrane filter from graphene oxide(GO) and banana rachis cellulose nano crystal(CNC) for industrial effluent treatment. *J. Indust. Eng. Chem.* 128, 196–208. <https://doi.org/10.1016/J.JIEC.2023.07.048>.
- Shelare, S.D., Belkhode, P.N., Nikam, K.C., Jathar, L.D., Shahapurkar, K., Soudagar, M.E. M., Veza, I., Khan, T.M.Y., Kalam, M.A., Nizami, A.S., Rehan, M., 2023. Biofuels for a sustainable future: Examining the role of nano-additives, economics, policy, internet of things, artificial intelligence and machine learning technology in biodiesel production. *Energy* 282, 128874. <https://doi.org/10.1016/j.energy.2023.128874>.
- Sheltami, R.M., Abdullah, I., Ahmad, I., Dufresne, A., Kargazadeh, H., 2012. Extraction of cellulose nanocrystals from mengkuang leaves (*Pandanus tectorius*). *Carbohydr. Polym.* 88, 772–779. <https://doi.org/10.1016/j.carbpol.2012.01.062>.
- Shen, F., Xiao, W., Lin, L., Yang, G., Zhang, Y., Deng, S., 2013. Enzymatic saccharification coupling with polyester recovery from cotton-based waste textiles by phosphoric acid pretreatment. *Bioresour. Technol.* 130, 248–255. <https://doi.org/10.1016/J.BIOTECH.2012.12.025>.
- Soudagar, M.E.M., Upadhyay, V.V., Naga Bhooshanam, N., Kumar, N., Venkatesh, R., Prabagaran, S., Wei, H., Al Obaid, S., Alharbi, S.A., 2024d. Enrichment of Chlorophytia growth via cerium oxide and utilized for hydrogen production via hydrothermal gasification process. *ASME. J. Energy Resour. Technol.* <https://doi.org/10.1115/1.4066762>.
- Soudagar, M.E.M., Kiong, T.S., Jathar, L., Ghazali, N.N.N., Ramesh, S., Awasarmol, U., Ong, H.C., 2024a. Perspectives on cultivation and harvesting technologies of microalgae, towards environmental sustainability and life cycle analysis. *Chemosphere* 353, 141540. <https://doi.org/10.1016/j.chemosphere.2024.141540>.
- Soudagar, M.E.M., Kiong, T.S., Ramesh, S., et al., 2024b. Utilization of non-edible bio-feedstock Pongamia Pinnata-diethyl ether ternary fuel blend supplemented with graphene oxide nanoparticles on CRDi engine characteristics. *J. Therm. Anal. Calorim.* 149, 5687–5712. <https://doi.org/10.1007/s10973-024-13143-2>.
- Soudagar, M.E.M., Shelare, S., Marghadie, D., Belkhode, P., Nur-E-Alam, M., Kiong, T.S., Ramesh, S., Rajabi, A., Venu, H., Khan, T.M.Y., Mujtaba, M.A., Shahapurkar, K., Kalam, M.A., Fattah, I.M.R., 2024c. Optimizing IC engine efficiency: a comprehensive review on biodiesels, nanofluid, and the role of artificial intelligence and machine learning. *Energy Convers. Manage.* 307, 118337. <https://doi.org/10.1016/j.enconman.2024.118337>.
- Teo, H.L., Wahab, R.A., 2020. Towards an eco-friendly deconstruction of agro-industrial biomass and preparation of renewable cellulose nanomaterials: a review. *Int. J. Biol. Macromol.* 161, 1414–1430. <https://doi.org/10.1016/j.ijbiomac.2020.08.076>.
- Thakur, M., Shamra, A., Ahlawat, V., Bhattachary, M., Goswami, S., 2020. Process optimization for the production of cellulose nanocrystals from rice straw derived a-cellulose. *Mater. Sci. Energy Technol.* 3, 328–334. <https://doi.org/10.1016/j.mset.2019.12.005>.
- Trache, D., Tarchoun, A.F., Derradj, M., Hamidon, T.S., Masruchin, N., Brosse, N., Hussin, M.H., 2020. Nanocellulose: from fundamentals to advanced applications. *Front. Chem.* 8. <https://doi.org/10.3389/fchem.2020.00392>.
- Uddin, M.J., Yeasmin, M.S., Muzahid, A.A., Rahman, M.M., Rana, G.M.M., Chowdhury, T.A., Al-Amin, M., Wakil, M.K., Begum, S.H., 2024. Morphostructural studies of pure and mixed metal oxide nanoparticles of Cu with Ni and Zn. *Heliyon* 10, e30544. <https://doi.org/10.1016/j.heliyon.2024.e30544>.
- Ulaganathan, R.K., Mohamad Senusi, N.A., Mohd Amrin, M.A., Abdul Razab, M.K.A., Ismardi, A., Abdullah, N.H., 2022. Effect of cellulose nanocrystals (CNC) on PVA/CNC bio nanocomposite film as potential food packaging application. *Mater. Today: Proc.* 66, 3150–3153. <https://doi.org/10.1016/J.MATPR.2022.07.466>.
- Wang, H., Xie, H., Du, H., Wang, X., Liu, W., Duan, Y., Zhang, X., Sun, L., Zhang, X., Si, C., 2020. Highly efficient preparation of functional and thermostable cellulose nanocrystals via H₂SO₄ intensified acetic acid hydrolysis. *Carbohydr. Polym.* 239, 116233. <https://doi.org/10.1016/J.CARBPOL.2020.116233>.
- Wunderlich, B., 2001. Thermal Analysis. *Encyclopedia of Materials: Science and Technology*, pp. 9134–9141. <https://doi.org/10.1016/B0-08-043152-6/01648-X>.
- Xie, H., Zou, Z., Du, H., Zhang, X., Wang, X., Yang, X., Wang, H., Li, G., Li, L., Si, C., 2019. Preparation of thermally stable and surface-functionalized cellulose nanocrystals via mixed H₂SO₄/Oxalic acid hydrolysis. *Carbohydr. Polym.* 223, 115116. <https://doi.org/10.1016/J.CARBPOL.2019.115116>.
- Zhao, Y., Liu, S., Xu, H., 2023. Effects of microplastic and engineered nanomaterials on inflammatory bowel disease: a review. *Chemosphere* 326, 138486. <https://doi.org/10.1016/J.CHEMOSPHERE.2023.138486>.
- Zor, M., Şen, F., Yazıcı, H., Candan, Z., 2023. Thermal, mechanical and morphological properties of cellulose/lignin nanocomposites. *Forests*. 14. <https://doi.org/10.3390/f14091715>.
- Żukowski, W., Jankowski, D., Wrona, J., Berkowicz-Platek, G., 2023. Combustion behavior and pollutant emission characteristics of polymers and biomass in a bubbling fluidized bed reactor. *Energy* 263, 125953. <https://doi.org/10.1016/J.ENERGY.2022.125953>.